AD-A164 187 REMOTE SENSING OF ATMOSPHERIC WINDS BY UTILIZING SPECKLE-TURBULENCE INTER..(U) OREGON GRADUATE CENTER BEAVERTON J F HOLMES ET AL. 21 NOV 85 ARO-20218.2-GS

1/1

UNCLASSIFIED DAAG29-83-K-0077 F/G 4/2 NL

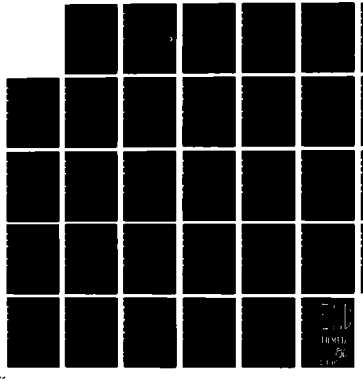

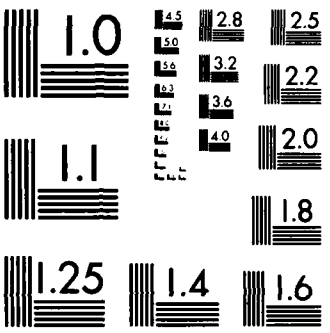

UNCLASSIFIED
SECURITY CLASSIFICATION OF THIS PAGE (When Data Entered)

(2)

MASTER COPY - FOR REPRODUCTION PURPOSES

REPORT DOCUMENTATION PAGE		READ INSTRUCTIONS BEFORE COMPLETING FORM
1. REPORT NUMBER ARO 20218.2-GS	2. GOVT ACCESSION NO. N/A	3. RECIPIENT'S CATALOG NUMBER N/A
4. TITLE (and Subtitle) Remote Sensing of Atmospheric Winds by Utilizing Speckle-turbulence Interaction and Optical Heterodyne Detection		5. TYPE OF REPORT & PERIOD COVERED Final 6/01/83 to 9/30/85 6. PERFORMING ORG. REPORT NUMBER N/A
7. AUTHOR(s) J. Fred Holmes		8. CONTRACT OR GRANT NUMBER(s) DAAG29-83-K-0077
9. PERFORMING ORGANIZATION NAME AND ADDRESS Oregon Graduate Center 19600 N.W. Von Neumann Drive Beaverton, OR 97006-1999		10. PROGRAM ELEMENT, PROJECT, TASK AREA & WORK UNIT NUMBERS N/A
11. CONTROLLING OFFICE NAME AND ADDRESS U. S. Army Research Office Post Office Box 12211 Research Triangle Park, NC 27709		12. REPORT DATE November 21, 1985 13. NUMBER OF PAGES 66
MONITORING AGENCY NAME & ADDRESS (if different from Controlling Office) N/A		15. SECURITY CLASS. (of this report) Unclassified 15a. DECLASSIFICATION DOWNGRADING SCHEDULE

AD-A164 187

DISTRIBUTION STATEMENT (of this Report)

Approved for public release; distribution unlimited.

DTIC ELECTE FEB 11 1986 S D B

DISTRIBUTION STATEMENT (of the abstract entered in Block 20, if different from Report)

NA

18. SUPPLEMENTARY NOTES

The view, opinions, and/or findings contained in this report are those of the author(s) and should not be construed as an official Department of the Army position, policy, or decision, unless so designated by other documentation.

19. KEY WORDS (Continue on reverse side if necessary and identify by block number)

Optical, Remote Sensing, Atmosphere, Winds, Speckle, Turbulence, Optical Heterodyne

DTIC FILE COPY

20. ABSTRACT (Continue on reverse side if necessary and identify by block number)

Speckle-turbulence interaction has the potential for allowing single ended remote sensing of the path averaged vector crosswind in a plane perpendicular to the line of sight to a target. If a laser transmitter is used to illuminate a target, the resultant speckle field generated by the target is randomly perturbed by the atmospheric turbulence as it propagates back to the location of the transmitter-receiver. When a crosswind is present, this scintillation pattern will move with time across the receiver-

DD FORM 1 JAN 73 1473 EDITION OF 1 NOV 65 IS OBSOLETE

UNCLASSIFIED
SECURITY CLASSIFICATION OF THIS PAGE (When Data Entered)

20. Abstract (continued)

aperture; and consequently, the time delayed statistics of the speckle field at the receiver are dependent on the crosswind velocity.

A continuous wave (cw) laser transmitter of modest power level (a watt or two) in conjunction with optical heterodyne detection has been used to exploit the speckle-turbulence interaction and measure the crosswind. The use of a cw transmitter at 10.6 microns and optical heterodyne detection has many advantages over direct detection and a double pulsed source in the visible or near infrared. These advantages include the availability of compact, reliable and inexpensive transmitters; better penetration of smoke, dust and fog; stable output power; low beam pointing jitter; and considerably reduced complexity in the receiver electronics. In addition, with a cw transmitter, options exist for processing the received signals for the crosswind that do not require a knowledge of the strength of turbulence.

During the period of this grant, an optical heterodyne transmitter-receiver system, using a CO_2 waveguide laser as a source, was designed and built. Several important results were obtained with the system including experimental proof that for coherent detection and a diffuse target, the peak of the time delayed covariance function does shift with crosswind as required for crosswind measurement. Reciprocity relationships for use with time delayed statistics were developed and verified, and the crosswind and strength of turbulence was remotely sensed.

Wind and turbulence strength measurements were made at 500 meter and 1000 meter ranges. The results are encouraging and have very positive implications with respect to remote sensing of winds and turbulence in the atmosphere.

ARO 20218.2-GS

Remote Sensing of Atmospheric Winds by Utilizing Speckle-Turbulence Interaction and Optical Heterodyne Detection

by

J. Fred Holmes

November 21, 1985

U.S. Army Research Office

Contract: DAAG29-83-K-0077

Oregon Graduate Center

19600 N.W. Von Neumann Drive

Beaverton, OR 97006-1999

(503) 690-1121

The view, opinions, and/or findings contained in this report are those of the author(s) and should not be construed as an official Department of the Army position, policy, or decision, unless so designated by other documentation.

Oregon Graduate Center

Final Technical Report

Remote Sensing of Atmospheric Winds by Utilizing Speckle-Turbulence Interaction and Optical Heterodyne Detection

Sponsor: Army Research Office

Contract Number: DAAG29-83-K-0077

Effective Date of Contract: June 1, 1983

Contract Expiration Date: September 30, 1985

Principal Investigator: Dr. J. Fred Holmes

Co-Principal Investigator: Dr. V. S. Rao Gudimetla

Senior Engineer: John M. Hunt

Student Research Assistants: Farzin Amzajerdian

Douglas Draper

Project Monitor: Dr. Walter A. Flood, ARO

SUMMARY

Speckle-turbulence interaction has the potential for allowing single ended remote sensing of the path averaged vector crosswind in a plane perpendicular to the line of sight to a target. If a laser transmitter is used to illuminate a target, the resultant speckle field generated by the target is randomly perturbed by the atmospheric turbulence as it propagates back to the location of the transmitter-receiver. When a crosswind is present, this scintillation pattern will move with time across the receiver aperture; and consequently, the time delayed statistics of the speckle field at the receiver are dependent on the crosswind velocity.

A continuous wave (cw) laser transmitter of modest power level (a watt or two) in conjunction with optical heterodyne detection has been used to exploit the speckle-turbulence interaction and measure the crosswind. The use of a cw transmitter at 10.6 microns and optical heterodyne detection has many advantages over direct detection and a double pulsed source in the visible or near infrared. These advantages include the availability of compact, reliable and inexpensive transmitters; better penetration of smoke, dust and fog; stable output power; low beam pointing jitter; and considerably reduced complexity in the receiver electronics. In addition, with a cw transmitter, options exist for processing the received signals for the crosswind that do not require a knowledge of the strength of turbulence.

During the period of this grant, an optical heterodyne transmitter-receiver system, using a CO_2 waveguide laser as a source, was designed and built. Several important results were obtained with the system including experimental proof that for coherent detection and a diffuse target, the peak of the time delayed covariance function does shift with crosswind as

required for crosswind measurement. Reciprocity relationships for use with time delayed statistics were developed and verified, and the crosswind and strength of turbulence was remotely sensed.

Wind and turbulence strength measurements were made at 500 meter and 1000 meter ranges. The results are encouraging and have very positive implications with respect to remote sensing of winds in the atmosphere.

TABLE OF CONTENTS

Introduction

Speckle-turbulence interaction has the potential for allowing single ended, remote sensing of the path averaged, vector crosswind. If a laser transmitter is used to illuminate a target (Figure 1), the resultant speckle field g ated by the target is randomly perturbed by the atmosphere as it propagates back to the receiver. This creates a scintillation pattern at the receiver; and, if a crosswind is present, this pattern will move across the field of view of the receiver. Consequently, the time delayed statistics of the speckle field at the receiver are dependent on the crosswind velocity and can be used to determine the vector crosswind in a plane perpendicular to the propagation direction.

As will be discussed below, we have previously accomplished some work on remote crosswind sensing utilizing speckle-turbulence interaction, a polychromatic source and direct detection.[1-8] This work was done in the near infrared utilizing a Nd:YAG laser operating at 1.06 microns. With a direct detection receiver, a pulsed transmitter is required; and furthermore, in order to measure the time delayed statistics, the transmitter must be double pulsed. This resulted in a complicated and very expensive transmitter that was plagued by beam alignment, beam jitter, stability and reliability problems. Nevertheless, some good experimental data that indicates the speckle-turbulence technique has merit was obtained.

Examples of this data are shown in Figures 2 and 3. The data was taken at the Biggs Optical Test Range (BOTR) in El Paso, Texas. In situ instrumentation consisted of a linear array of 20 propeller anemometers spaced evenly along the path. Their outputs were added without weighting to provide the solid trace. The output of the pulsed system is shown by the dashed lines. A four second averaging time was used.

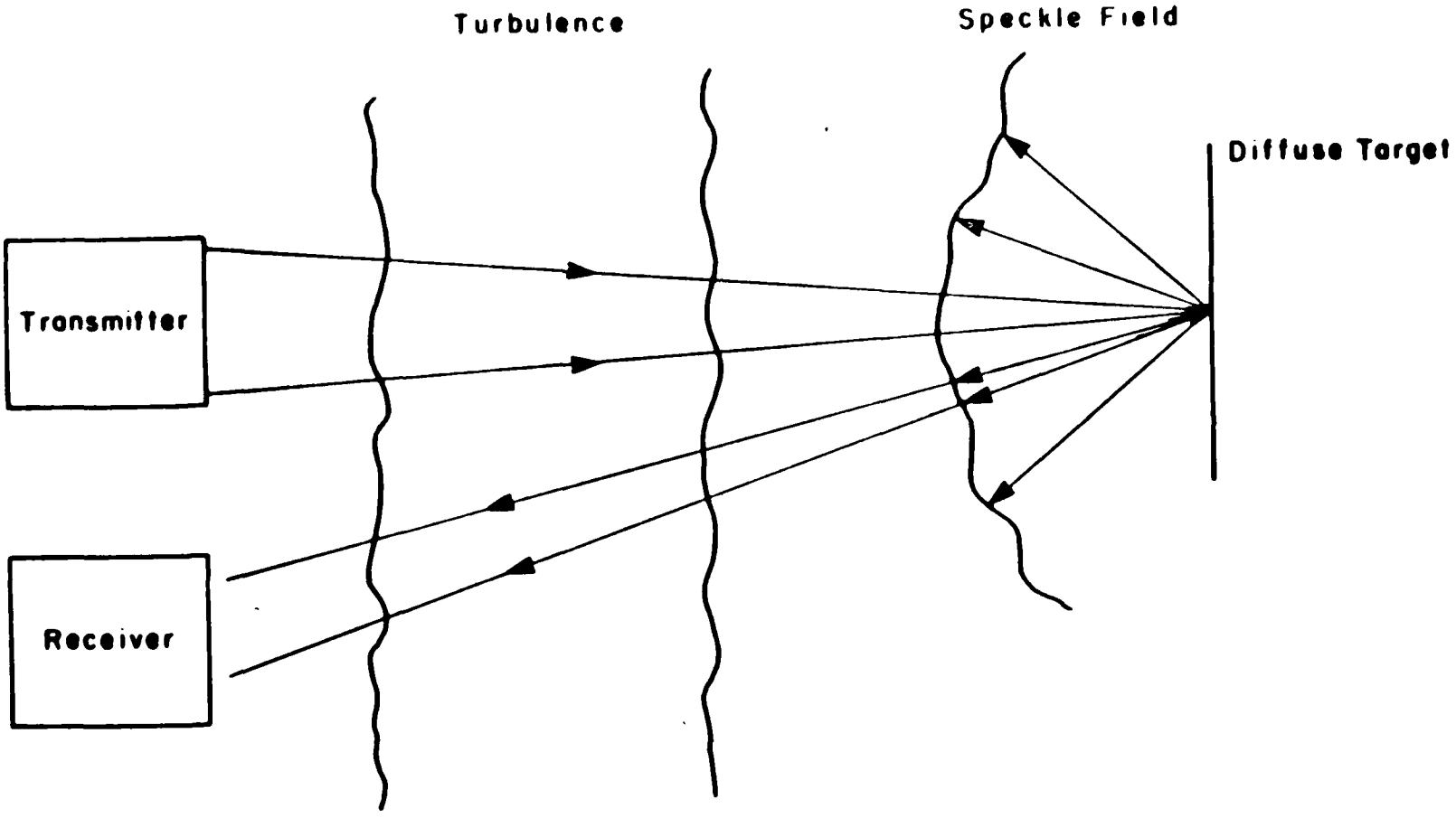

FIGURE 1. TRANSMITTER-RECEIVER

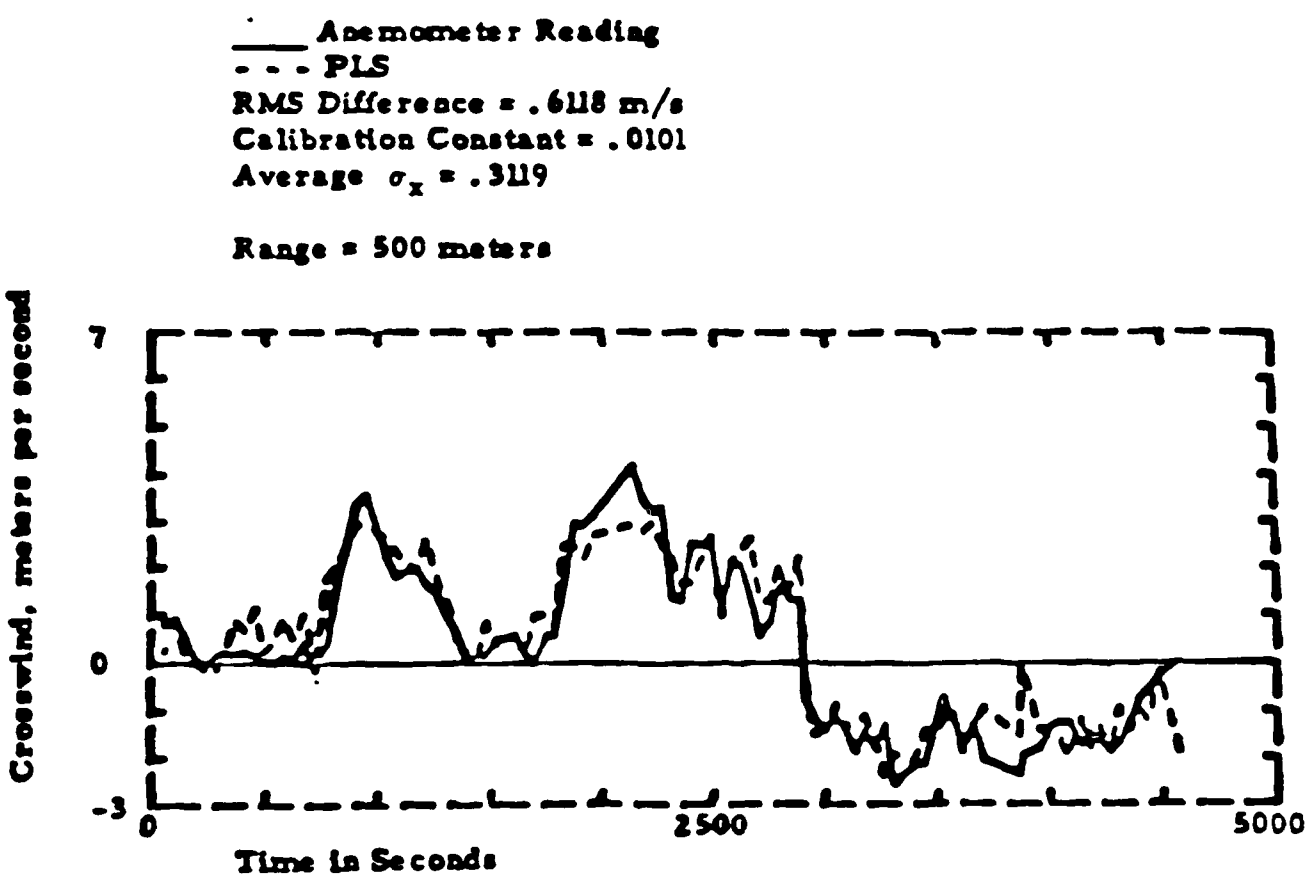

Figure 2. Wind measurement pulsed laser system.

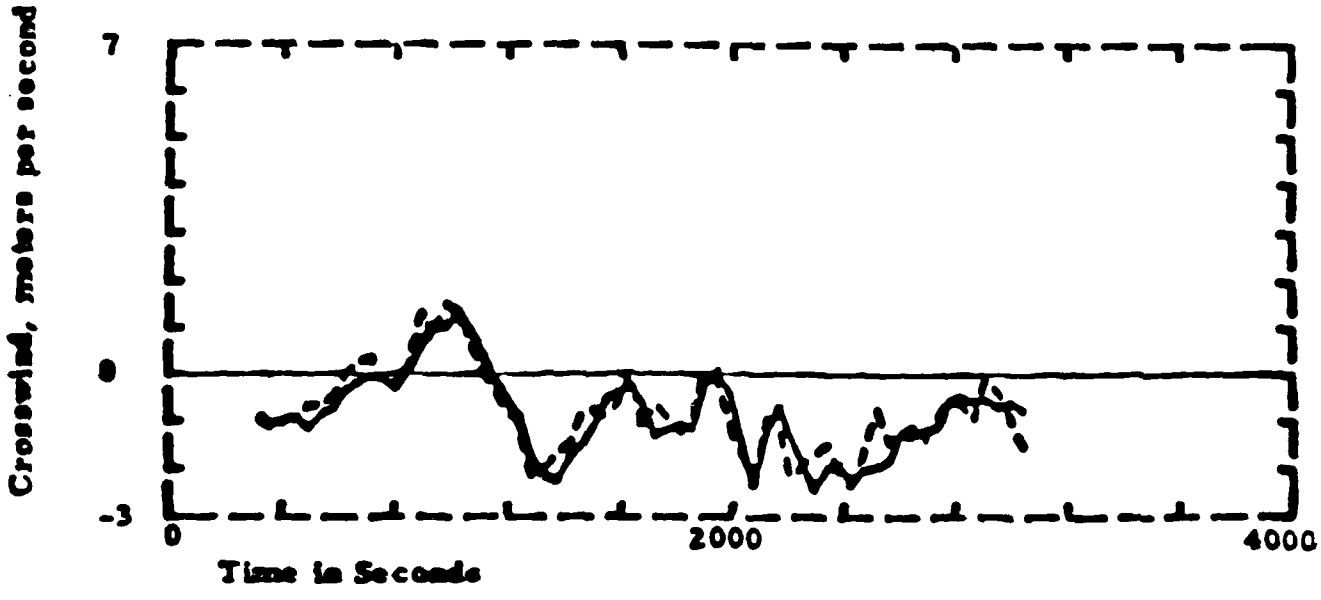

Figure 3. Wind measurement pulsed laser system.

The key features of the direct detection system were:

- Pulsed Laser
- Polychromatic
- Direct Detection
- 1.06 Microns Wavelength

Although good results were obtained with this system, it has a fatal flaw. Because of the limited pulse repetition rate, the only usable processing technique is the slope of the time lagged covariance function at zero time delay. However the slope is proportional to both the crosswind and the strength of turbulence. Since the strength of turbulence is not known a priori, the system will not be useful until there are significant improvements in pulsed laser technology that will allow other signal processing methods to be used that do not require an a priori knowledge of the strength of turbulence.

A continuous wave (cw) laser transmitter of modest power level in conjunction with optical heterodyne detection can be used to exploit the speckle-turbulence interaction and measure the crosswind. The key features of such systems are:

- Continuous Wave
- Monochromatic
- Heterodyne Detection
- 10.6 Microns Wavelength

which is just about the opposite of the features for the 1.06 micron system.

The use of a cw transmitter at 10.6 microns and optical heterodyne detection has many advantages over direct detection and a double pulsed source in the visible or near infrared. These advantages include the availability of compact, reliable and inexpensive transmitters; better penetration of smoke, dust and fog; stable output power; low beam pointing jitter; and considerably

reduced complexity in the receiver electronics. In addition, with a cw transmitter, options exist for processing the received signals for the crosswind that do not require a knowledge of the strength of turbulence, the fatal flaw of the 1.06 microns system. During the period of this research grant, an optical heterodyne transmitter-receiver system, using a CO_2 waveguide laser as a source, was designed and built. Several important results were obtained with the system including experimental proof that for coherent detection and a diffuse target, the peak of the time delayed covariance function does shift with crosswind as required for crosswind measurement. A reciprocity relationship for use with time delayed statistics was developed and verified, and the crosswind and strength of turbulence remotely sensed.

Wind and turbulence strength measurements were made at 500 meter and 1000 meter ranges. The results are encouraging and have very positive implications with respect to remote sensing of winds in the atmosphere.

Background

Analytic formulations for the first and second order statistics of the received intensity have been developed for the case where a diffuse target is illuminated by a TEM_{00} monochromatic laser beam.[9-11] They properly account for the effect of atmospheric turbulence both for propagation of the laser beam from the transmitter to the target and propagation of the target induced speckle field back to the receiver. The exact formulations are quite complex and difficult to interpret. However, for longer wavelength sources such as 10.6 microns, simple formulations based on the joint Gaussian assumption are valid for almost all physically realizable scenarios.

From previous work, the time delayed covariance function using the joint Gaussian assumption is given for the focused case by[9]

$$C_I(\overline{P},\tau) = \langle [I(\overline{P}_2, t_2) - \langle I \rangle][I(\overline{P}_1, t_1) - \langle I \rangle] \rangle \quad (1)$$

$$= \langle I \rangle^2 \exp\left[- \frac{P^2}{2\alpha_o^2} - \frac{32}{3\rho_o^{5/3}} \int_0^1 \left| (1-w)\overline{P} - \overline{V}\tau \right|^{5/3} dw \right] \quad (2)$$

where $\overline{P}_i$ designates the location of a detector in the receiver plane,

$\overline{P} = \overline{P}_2 - \overline{P}_1$

$\tau = t_2 - t_1$

α_o = Transmitter Beam Radius

ρ_o = Transverse Phase Coherence Length

$\overline{V}$ = Vector Wind Velocity

and

W = Normalized Path Length from the Transmitter-Receiver to the Target.

As can be seen from Eq.(1), if two detectors are separated by a vector distance $\overline{P}$, the time delayed covariance can be measured; and from Eq.(2) it can be seen that the measured quantity will be a function of the crosswind velocity.

With a cw system there are several options for processing the data to obtain the wind. Some of these methods are illustrated in Figure 4. The Briggs method measures the time delay, τ_B, at which the autocovariance and the time-lagged covariance curves cross. The delay to peak method, measures the time delay, τ_p, where the time-lagged covariance reaches its peak value. The width of the autocovariance method measures the time delay, τ_w, at which the autocovariance curve decreases to 67% of its peak value. the slope method measures the slope, S, of the time-lagged covariance function at zero time delay. All of these methods have been used for the line of sight

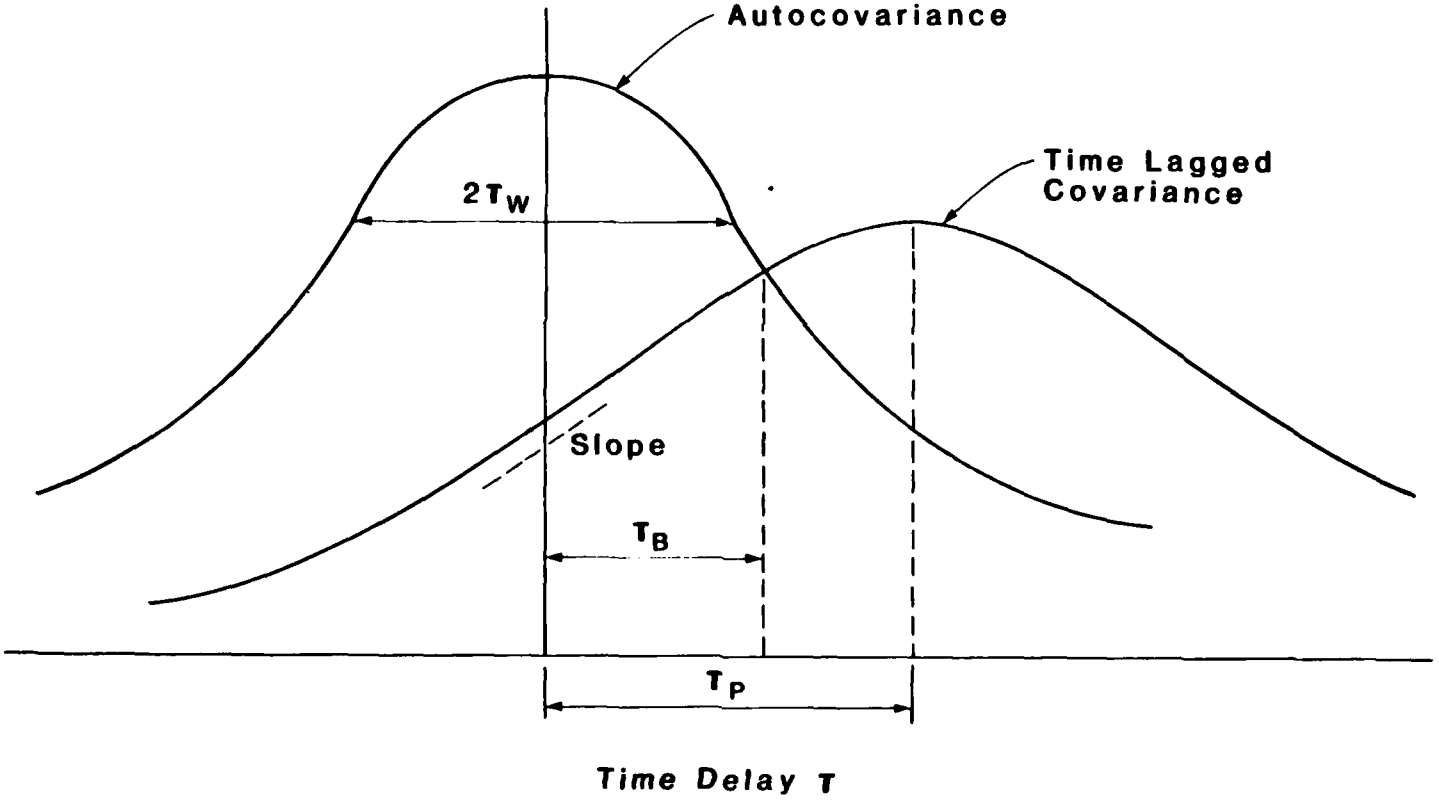
Autocovariance
Time Lagged
Covariance
2Tw
Slope
TB
TP
Time Delay τ

Figure 4

case and appear to have applicability to remote wind sensing using speckle turbulence interaction. Assuming uniform wind and turbulence, the wind velocity for these methods is given by

- Briggs Method

$$V = \frac{P}{3.1056\,\tau_B}$$

- Delay to Peak Method

$$V = \frac{P}{2\tau_P}$$

- Width of Autocovariance Method (67%)

$$\frac{V}{\rho_o} = \frac{0.1395}{\tau_W}$$

- Slope

$$V = \frac{3}{32}\,\frac{\rho_o^{5/3}}{P^{2/3}}\,\frac{S}{C_I(\bar{\rho},o)}$$

The above techniques were not evaluated during the period of this report due to time constraints. However, during the next year or so, it is planned to evaluate the usefulness of each of these techniques. Some new methods have been developed that use both the autocovariance function and the time lagged covariance. Formulation for these quantities are functions of both the crosswind and ρ_o the transverse phase coherence length. By combining them and also averaging the results for several different time delays, both the crosswind and ρ_o can be measured. One result for the crosswind which was used to process the data presented in a later section is

$$V = \frac{1}{N} \sum_{i=1}^{N} \frac{P}{\tau_i} \left[\frac{\ell n\, C_{IN}(o, \bar{v}\, \tau_i)}{\ell n\, C_{IN}(\bar{P}, o) + p^2 / 2\alpha_o^2} \right]^{3/5} \qquad (3)$$

where

P = detector spacing

α_o = Beam Radius

τ_i = i^{th} time delay

C_{IN} = Normalized (to the mean squared) time lagged covariance

N = Number of time delays used

and where the direction of the crosswind is determined by the skewness of the TLC. There are other variations on this approach; but better data is needed for evaluation. The number of time delays used for the data processed was typically five.

Experimental Apparatus

The transmitter optics is shown in Figure 5. The source is a CO_2 waveguide laser. Part of the laser radiation is split from the main beam and focused onto the two detectors for use as an optical local oscillator. The remaining part of the beam is directed through an acoustooptic modulator (AO) where its optical frequency is shifted by 37.5 MHz and then passed through a 40 X beam expander that is focused on the target. The half-wave plate rotates the polarization of the beam from vertical to horizontal to match the AO modulator and the quarter-wave plate provides a circularly polarized output beam.

The transmitter beam is scattered diffusely by a 4 foot × 4 foot sandblasted aluminum target. The returning radiation is directed by two one-inch mirrors onto lenses that focus it on the detectors. The effective area of the receivers is approximately one-half square inch and the transmitted power is around one watt.

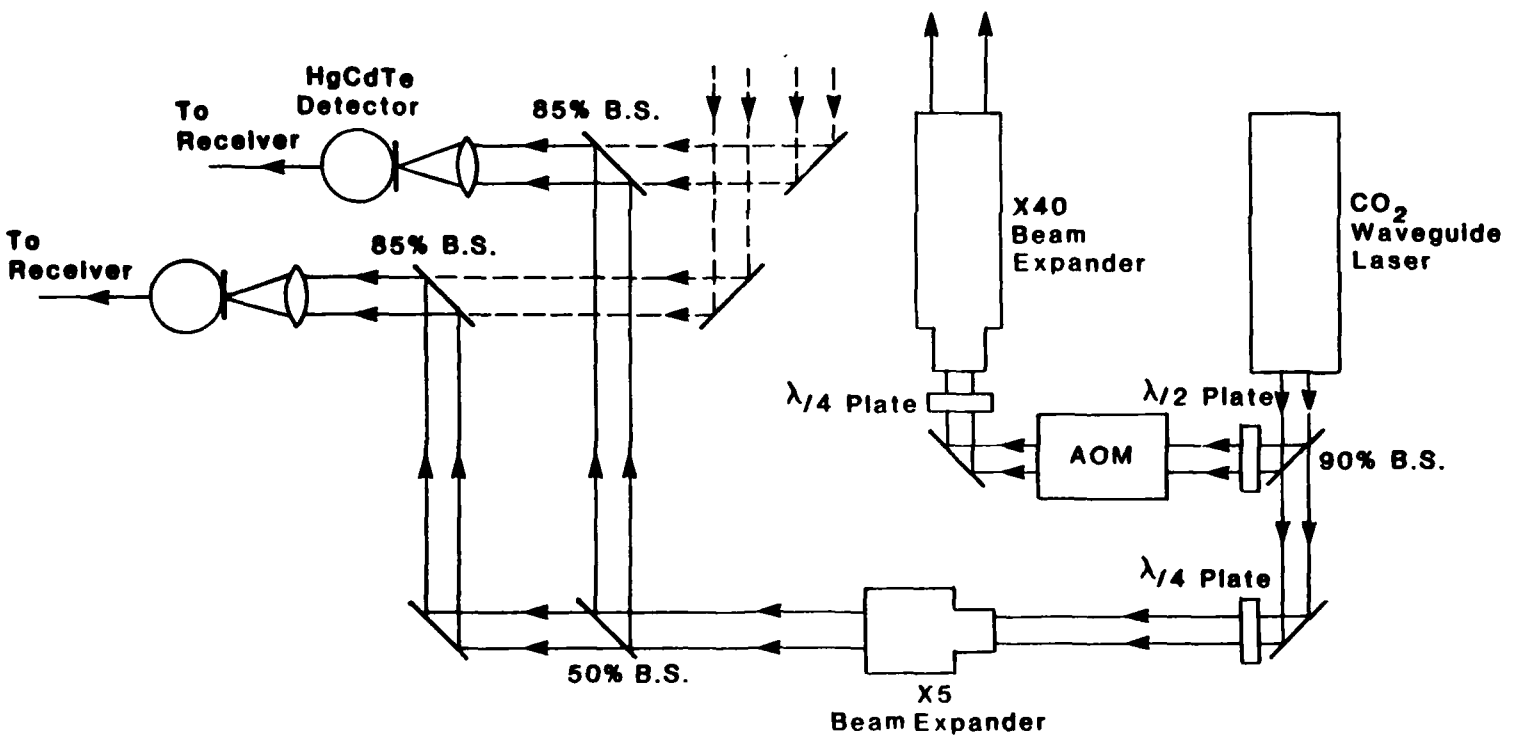

Figure 5. Transmitter Optics

The main problem encountered in using the system was optical feedback of the transmitted beam to the detectors. The source of the feedback is the acoustooptic modulator. Apparently there is some diffuse scattering of both the unshifted and frequency shifted light by the germanium crystal used in the modulator. Even though there is around 100 db of isolation, the levels fed back are sufficient to cause large homodyne type amplitude beats on the heterodyne signal. The feedback light causes two problems: when it is detected it creates a DC offset that makes processing for the statistics difficult; and it also mixes with the actual signal from the target which generates large amplitude homodyne beats.

The optical feedback problem was not anticipated and a great deal of effort was made to eliminate it. By using quarter-wave plates and Brewster angle polarizers the problem was reduced to a point where some useful but still contaminated data could be obtained. Unfortunately, the polarization of the optical feedback was not stable; and so the degree of isolation would vary over time. Frequent readjustment was required.

Two solutions were proposed for the problem: a gated cw transmitter; and the use of separate lasers for the transmitter and local oscillator. By using the time delay inherent in the transmitted wave traveling to the target and back to the receiver, the transmitter and receiver can be synchronously turned on and off out of phase such that the optical feedback is not present on the receiver at the same time as the signal from the target. The laser actually runs cw for stability reasons and the transmitter switching is done with the acoustooptic modulator. It was expected that two to three orders of magnitude improvement would be obtained. However, only about a factor of 25 was achieved due to scattering from echoes in the acoustooptic (AO) modulator. The addition of a second AO modulator would significantly increase the isolation.

As mentioned above, the second approach uses separate lasers for the transmitter and LO. Since there is no common optical path, virtually complete isolation should be obtainable.

The method of gating the transmitter and receiver is illustrated in Figure 6. The transmitter was gated by switching the RF drive to the acoustooptic modulator and the receivers were gated by switching the RF local oscillator used to mix down the received signal at 37.5 MHz to the 5 MHz IF frequency. A block diagram of the receiver is shown in Figure 7. The data contained in the next section was taken with the switched cw system as described above.

Experimental Results

Representative experimental data with the target at 500 meters range is shown in Figures 8 through 10. Equation (3) was used for the processing and it should be noted that there are no arbitrary parameters used and that no a priori knowledge of the strength of turbulence is needed. These results are encouraging.

A small amount of data has been obtained with the target at 1000 meters. Since the signal is reduced at longer ranges; but the optical feedback remains constant, the quality of the data decreases. Figures 11 and 12 show some of the better sections of data for 1000 meters range. It is noted that there is some bias which may be caused by residual correlation from the optical feedback.

The in situ data for both the 500 meters and 1000 meters path length were obtained by using a Campbell Scientific, CA-9, path averaging crosswind sensor. It should be noted that the CA-9 and Heterodyne sensors have different path weighting functions which may account for some of the differences in indicated wind speed.

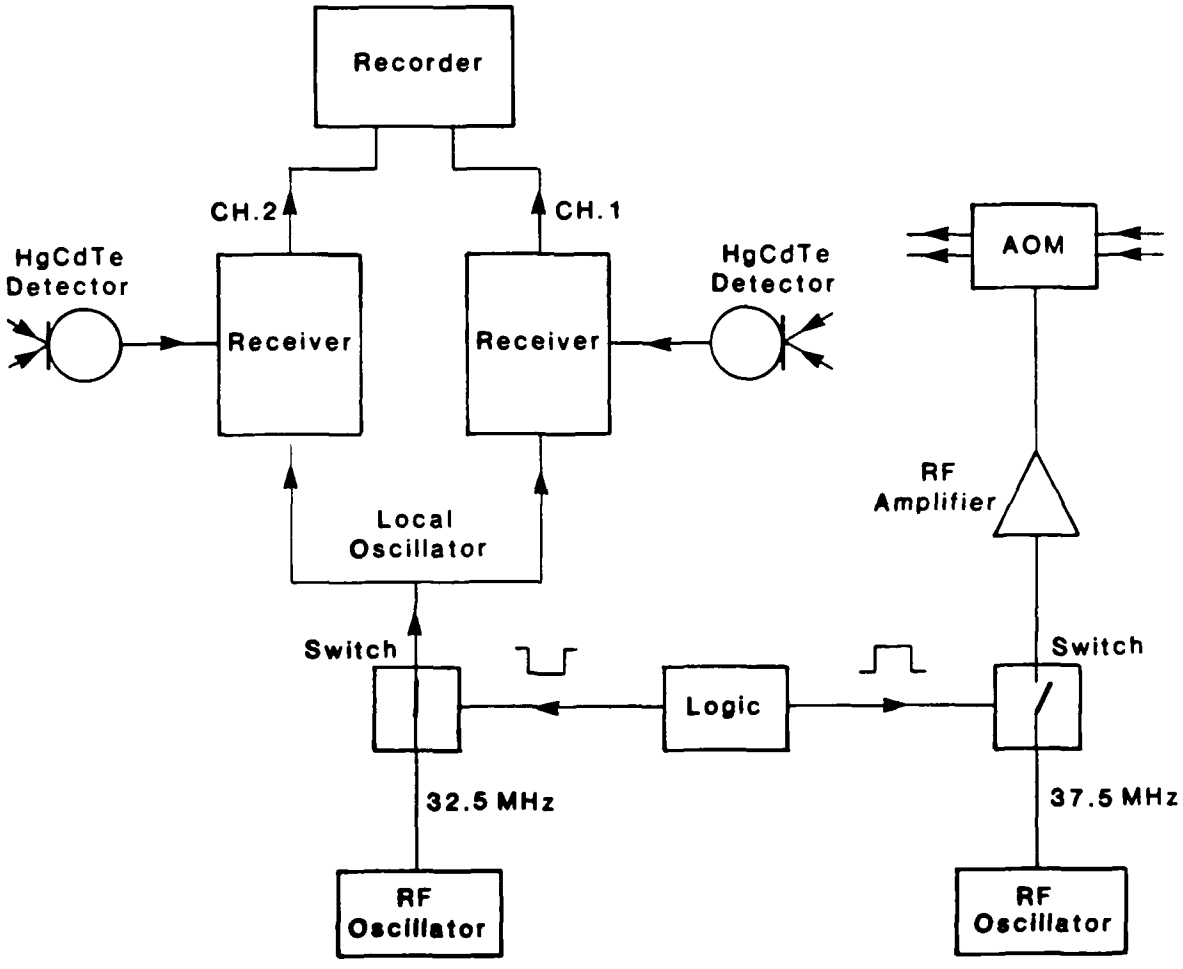

Figure 6. Transmitter Electronics

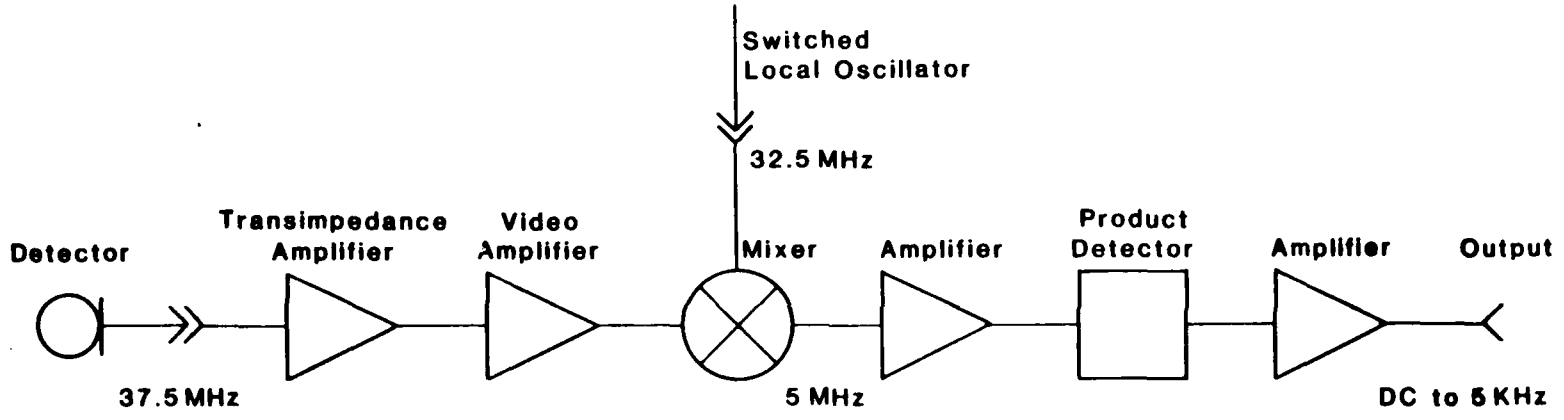

Figure 7. Receiver

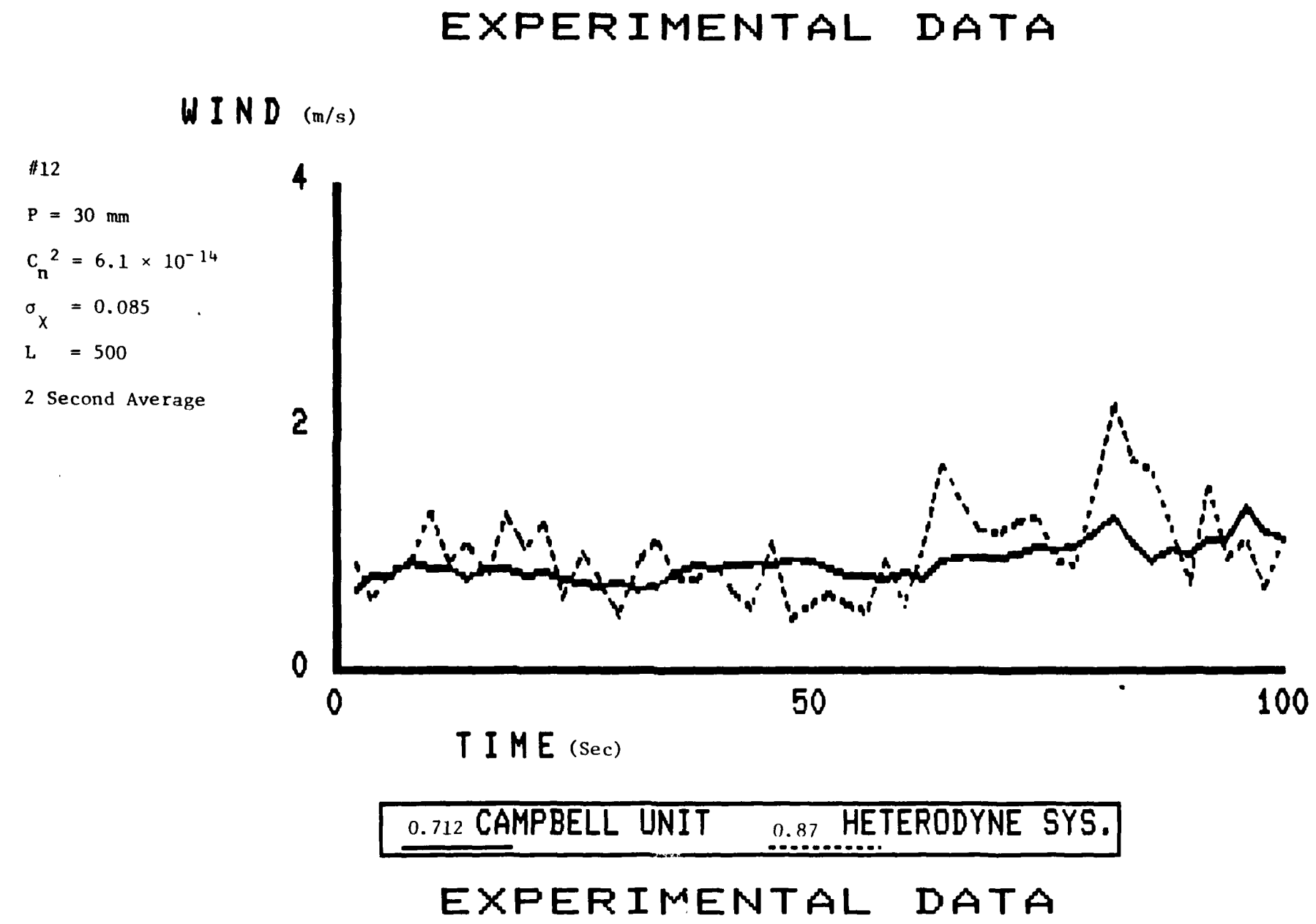

Figure 8. 500 meter Experimental Data
Wind = 0.712 m/s

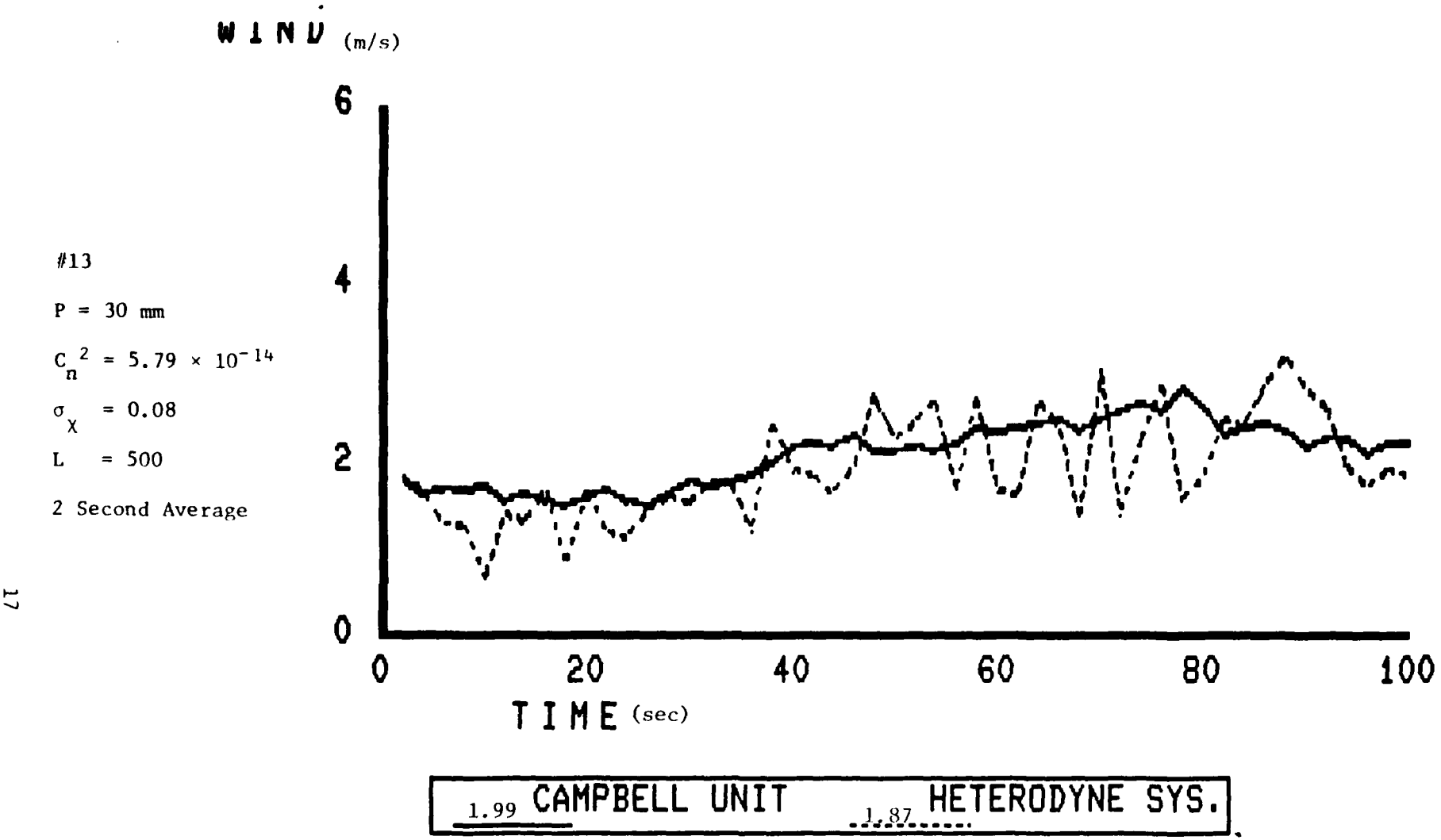

Figure 9. 500 meter Experimental Data
Wind = 1.99 m/s

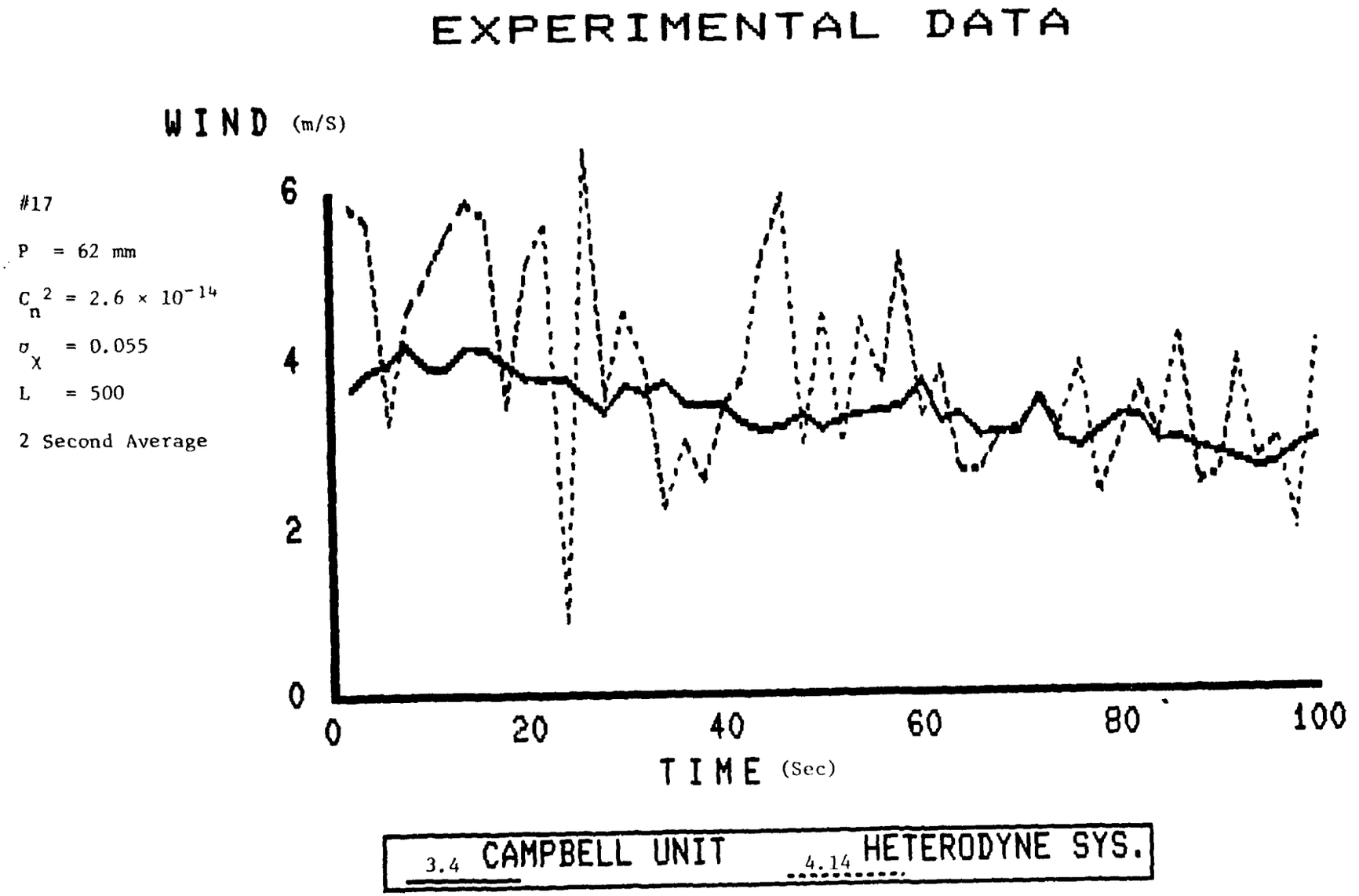

Figure 10. 500 meter Experimental Data
Wind = 3.4 m/s

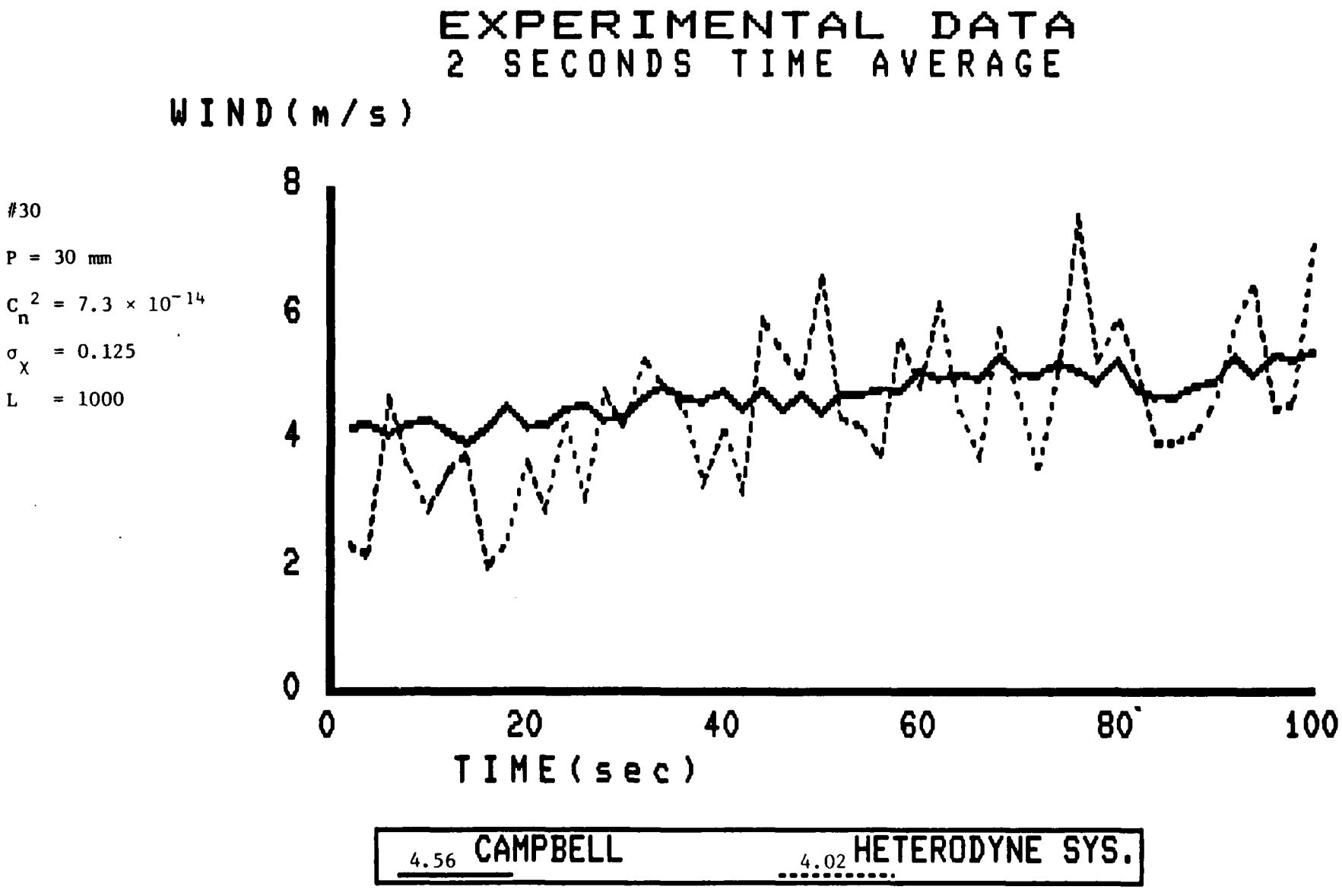

Figure 11. 1000 meter Experimental Data
Wind = 4.56 m/s

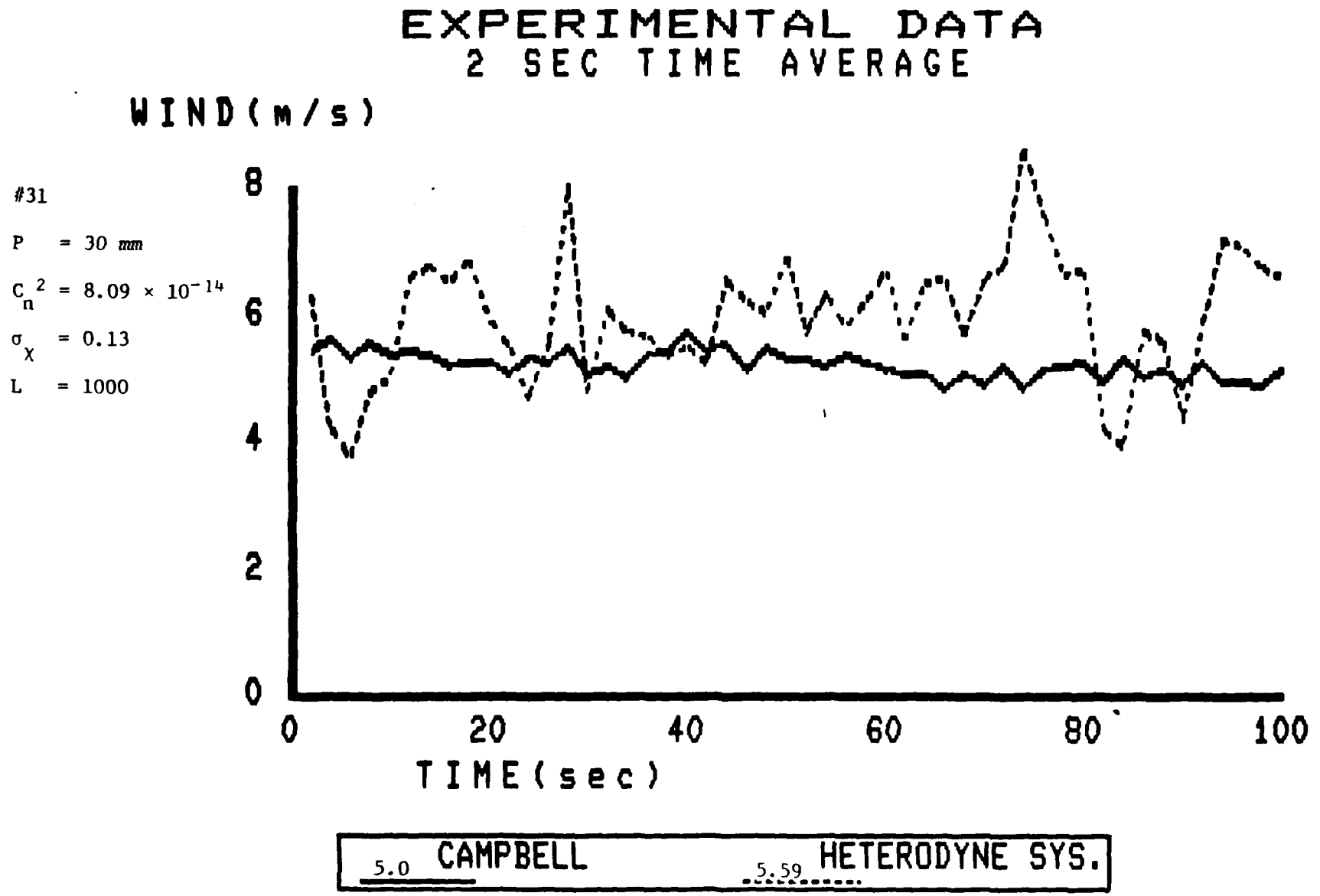

Figure 12. 1000 meter Experimental Data
Wind = 5.0 m/s

Publications and Conference Papers

V. S. Rao Gudimetla and J. Fred Holmes, "The Use of Reciprocity in Lidar Type Optical Propagation Problems Involving Time Delayed Statistics," submitted to Applied Optics.

J. Fred Holmes, Farzin Amzajerdian, V. S. Rao Gudimetla and John M. Hunt, "Remote crosswind measurement using speckle-turbulence interaction and optical heterodyne detection," Annual Meeting of the Optical Society of America, October 14-18, 1985, Washington, D.C.

(Invited) J. Fred Holmes, "The characteristics and effects of speckle propagation through turbulence," Optical Society of America Topical Meeting on Optical Remote Sensing of the Atmosphere, January 15-18, 1985, Incline Village, Nevada.

V. S. Rao Gudimetla and J. Fred Holmes, "Time Lagged Reciprocity in the Turbulent Atmosphere," Annual Meeting of the Optical Society of America, San Diego, CA, October 29-November 2, 1984.

J. Fred Holmes and V. S. Rao Gudimetla, "The Effects of Target and Source Motion and Beam Slewing on Speckle Propagation Through Turbulence," National Radio Science Meeting, January 11-14, 1984, Boulder, Colorado.

J. Fred Holmes and V. S. Rao Gudimetla, "Effects of Target and Source Motion on Speckle Propagation Through Turbulence," Annual Meeting of the Optical Society of America, New Orleans, LA, October 17-20, 1983.

The above papers were supported in part under this grant. Copies are contained in Appendix A.

Personnel Supported in Part by this Grant

Dr. J. Fred Holmes

Dr. V. S. Rao Gudimetla

Mr. John M. Hunt

Mr. Farzin Amzajerdian (Ph.D. Student)

Mr. Douglas C. Draper (Ph.D. Student)

References

1. (Invited) J. Fred Holmes, "A Single Ended System for Remote Crosswind Measurement in the Turbulent Atmosphere," German-French Research Institute (ISL) Symposium on Long Range and Short Range Optical Velocity Measurements, Saint-Louis, France, September 15-18, 1980.

2. J. Fred Holmes, Myung Hun Lee, Michael E. Fossey, "Remote Crosswind Measurement Utilizing the Interaction of a Target Induced Speckle Field with the Turbulent Atmosphere," Annual Meeting of the Optical Society of America, Chicago, Illinois, October 13-17, 1980.

3. J. Fred Holmes and Myung Lee, "Estimation of the Error in Remote Crosswind Sensing Caused by Atmospheric Turbulence and Speckle," Annual Meeting of the Optical Society of America, Kissimmee, Florida, October 26-30, 1981.

4. J. F. Holmes, et al., "Experimental Pulsed Laser, Remote Crosswind Measurement System -- Feasibility Study and Design," U.S. Army Electronics Command, Research and Development Technical Report ECOM 74-0094-1, Atmospheric Sciences Laboratory, U.S. Army Electronics Command, White Sands Missile Range, New Mexico 88002, July 1974.

5. J. F. Holmes, et al., "Experimental Pulsed Laser, Remote Crosswind Measurement System -- Feasibility Study and Design (Part II)," U.S. Army Electronics Command, Research and Development Technical Report ECOM75-1, Atmospheric Sciences Laboratory, U.S. Army Electronics Command, White Sands Missile Range, New Mexico 88002, January 1975.

6. J. F. Holmes, et al., "Experimental Pulsed Laser, Remote Crosswind Measurement System -- Feasibility Study and Design (Part III)," U.S. Army Electronics Command, Research and Development Technical Report ECOM75-1, Atmospheric Sciences Laboratory, U.S. Army Electronics Command, White Sands Missile Range, New Mexico 88002, September 1975.

7. J. F. Holmes, et al., "Experimental Pulsed Laser, Remote Crosswind Measurement System -- Feasibility Study and Design (Part IV)," U.S. Army Armament Command, Research and Development Technical Report FA-TA-76065, Frankford Arsenal, Philadelphia, PA 19137, November 1976.

8. J. F. Holmes, et al., "Experimental Pulsed Laser, Remote Crosswind Measurement System -- Feasibility Study and Design (Part V)," U.S. Army Armament Command, Research and Development Technical Report ARSCD-CR-79-007, Fire Control and Small Caliber Weapon Systems Laboratory, Dover, New Jersey, September 1978.

9. Myung Hun Lee, J. Fred Holmes, and J. Richard Kerr, "Statistics of speckle propagation through the turbulent atmosphere," J. Opt. Soc. Am. 66, November 1976.

10. Philip A. Pincus, Michael E. Fossey, J. Fred Holmes and J. R. Kerr, "Speckle propagation through turbulence - experimental," J. Opt. Soc. Am. 68, June 1978.

11. J. Fred Holmes, Myung Hun Lee, and J. Richard Kerr, "Effect of the log-amplitude covariance function on the statistics of speckle propagation through the turbulent atmosphere," J. Opt. Soc. Am. 70, April 1980.

APPENDIX A

Publications and Conference Papers

Submitted to the Journal of Applied Optics

The Use of Reciprocity in Lidar Type Optical Propagation Problems Involving Time Lagged Statistics

by

V. S. Rao Gudimetla

and

J. Fred Holmes

Department of Applied Physics and Electrical Engineering

Oregon Graduate Center, 19600 N.W. Von Neumann Drive

Beaverton, Oregon 97006-1999

(503) 645-1121

ABSTRACT

In optical propagation problems involving atmospheric turbulence and single ended transmitter-receiver systems, formulations for the time-lagged statistics will involve point spread functions representing optical propagation in both directions. In order to use these formulations, reciprocity must be used. However, for time lagged statistics, care must be exercised when using reciprocity. This paper shows how the reciprocity principle should be used in the case of time lagged statistics and presents experimental evidence to support the result.

Introduction

In single ended optical propagation problems in the turbulent atmosphere, the transmitter and receiver are located at the same end of the propagation path. The transmitted radiation propagates down the path and strikes a target where it is scattered or reflected back towards the receiver. This radiation interacts with the atmospheric turbulence on both the down and back paths. The reciprocity principle[1,2] says that if a point source at $\bar{r}$ in the transmitter plane generates a certain field at $\bar{\rho}$ in the receiver plane; and if the point source is moved to $\bar{\rho}$, it will then produce that same field at $\bar{r}$. It can be expressed in terms of the complex wave perturbation ψ due to a point source in the turbulent atmosphere as

$$\psi(\bar{r}, \bar{\rho}, t) = \psi'(\bar{\rho}, \bar{r}, t) \tag{1}$$

where the unprimed quantity refers to propagation from the transmitter/receiver plane source to the target and the primed quantity refers to propagation from the target plane back to the transmitter/receiver plane. Clearly, as long as the transit time is small with respect to the decorrelation time of the atmosphere, the reciprocity principle is valid. However Eq.(1) is symbolic and as will be shown, does not necessarily imply that formulations for ψ and ψ' can be used directly in it when dealing with problems that involve atmospheric propagation in both directions and time lagged statistics.

The complex wave perturbation can be used in the extended Huygens-Fresnel formulation to determine the fields at the receiver, including the effects of turbulence. This requires that the extended Huygens-Fresnel formulation be used twice, once for the path down and once for the path back.[3] Consequently, the final result for the field at the receiver will contain both ψ and ψ'. When this expression for the fields is used to evaluate the statistics at the receiver, the result will contain statistics for both ψ and '.

If the turbulence is isotropic, and homogeneous in the transverse plane, then the non-time lagged statistics will depend only on the magnitude of the vector distance between field points and no problems arise using Eq.(1).[4,5,6] However, when time-delayed statistics are considered and a crosswind is present, they will in general depend on the vector distance between field points and the statistics become anisotropic. Since vector results sometimes depend on the direction of propagation and the coordinate system,[7] care must be taken in using reciprocity when time-lagged statistics are considered and propagation in two directions are involved.

Figure 1 illustrates an example of the problem and will help lead to the solution. At the top of the figure is shown a correlation type of crosswind sensor on the left and a point source on the right. The sensor has two detectors labeled D2 and D1. The time lagged correlation then will peak for a positive

value of $\tau = t_2 - t_1$ and the instrument will indicate the crosswind velocity as V. However, if the crosswind sensor is now rotated about the y axis shown in Figure 2 and exchanged with the point source as shown in the lower part of Figure 1 it will indicate the crosswind as -V since D2 now sees the turbulence pattern before D1. To straighten things out, the crosswind sensor must also be rotated about the z axis. It will then indicate the correct value of crosswind but the sense of the actual wind with respect to the new coordinate system will be reversed. It appears then that in problems of this type, either the coordinates need to be reversed or the crosswind reversed in order for ψ and ψ' to be interchangeable through reciprocity; and that a correct reciprocity relationship to be used in single ended atmospheric propagation problems involving time lagged statistics is

$$\psi(\bar{r}, \bar{\rho}, t, \bar{V}) = \psi'(\bar{\rho}, \bar{r}, t, -\bar{V}) \quad . \tag{2}$$

At this point some readers may feel that Eq.(2) is obviously correct. However, for the skeptics, an experiment has been designed that has clearly different predicted results depending on whether Eq.(1) or Eq.(2) is used. First it will be shown analytically in the next section that Eq.(2) is correct, and then the predicted and experimental results will be presented. However, before proceeding it should be emphasized that Eq.(2) does not deny that reciprocity as implied symbolically by Eq.(1) is not valid. It only states that when the two propagation directions are mixed in a problem, that the wind velocity must be reversed in the reciprocity relationship.

Analytical Development

Although the problem being considered is not strictly time harmonic, the time harmonic solution to Maxwell's equations that leads[8] to a formulation for $\psi(\bar{r}, \bar{\rho}, t, \bar{v})$ can still be used because the index of refraction variations due to the atmospheric turbulence are small and vary slowly in time. The formulation is given by

$$\psi(\bar{r}, \bar{\rho}, t) = \frac{k^2}{2\pi} \exp\left[ik \frac{|\bar{r} - \bar{\rho}|^2}{2L} \right]$$

$$\cdot \int dx_1\, dy_1\, dz_1 \; n_1(\bar{r}_1, t) \exp\left[ik \left(\frac{|\bar{r} - \bar{r}_1|^2}{2z_1} + \frac{|\bar{\rho} - \bar{r}_1|^2}{2(L - z_1)} \right) \right] / [z_1 (L - z_1)] \tag{3}$$

where $n_1(\bar{r}_1, t, \bar{v})$ is the random part of the index of refraction and L is the distance from the transmitter to the target. If the source and field points are interchanged in (3) and it is transferred to the primed coordinate system, it becomes

$$\psi'(\bar{r}, \bar{\rho}, t) = \frac{k^2}{2\pi} \exp\left[ik \frac{|\bar{r} - \bar{\rho}|^2}{2L} \right]$$

$$\cdot \iint dx_1'\, dy_1'\, dz_1'\; n_1'(\bar{r}_1', t) \exp\left[ik \left(\frac{|\bar{r} - \bar{r}_1'|^2}{2z_1} + \frac{|\bar{\rho} - \bar{r}_1'|^2}{2(L - z_1')} \right) \right] / [(z_1'(L - z_1'))] \tag{4}$$

It can be seen from Eq.(4) that if the functional form for n_1' is the same as for n_1, then the functional form for ψ will be the same as for ψ' and they are interchangeable. Since for the problem of interest n_1 is approximately proportional to δT, the temperature deviation from the mean, the differential equation for δT will be used to determine the proper form of reciprocity to be used in problems involving propagation in both directions. The differential equation for δT is given by[9]

$$\frac{\partial \delta T}{\partial t} + V_x \frac{\partial \delta T}{\partial x} + V_y \frac{\partial \delta T}{\partial y} + V_z \frac{\partial \delta T}{\partial z} = \chi \nabla^2 \delta T \tag{5}$$

where χ is the thermal diffusivity and $\bar{V} = V_x\hat{x} + V_y\hat{y} + V_z\hat{z}$ represents the wind. Transferring Eq.(5) to the primed coordinate system it becomes

$$\frac{\partial \delta T'}{\partial t} - V_x \frac{\partial \delta T'}{\partial x'} - V_y \frac{\partial \delta T'}{\partial y'} - V_z \frac{\partial \delta T'}{\partial z'} = \chi \nabla'^2 \delta T' \tag{6}$$

It can be seen that if the wind field is reversed in Eq.(6), then it will be identical to Eq.(5) and consequently the functional form for n_1' will be identical to that for n_1. This is equivalent to expressing the wind field in the primed system. The proper relationship to be used then appears to be

$$\psi(\bar{r}_o, \bar{r}, t, \bar{V}) = \psi'(\bar{r}, \bar{r}_o, t, \bar{V}')$$

$$= \psi'(\bar{r}, \bar{r}_o, t, -\bar{V}) \tag{7}$$

In the next section, experimental results that support this contention will be presented.

Experimental Results

A CO_2 laser transmitter, a diffuse target and an optical heterodyne receiver have been used to measure the time-lagged covariance function of the intensity for an atmospheric propagation path. The transmitter and receiver are located on one end of the path and the target at the other end. Before presenting the experimental results, a previously derived formulation for the time-lagged covariance will be used to show that the result using Eq.(1) is clearly different from the result using Eq.(2).

For lower levels of turbulence, the time-lagged covariance for the focused case and within the limitations of Taylor's hypothesis is given by[3]

$$C_I = \left|\Gamma(\bar{P}_1, \bar{P}_2, \bar{V}\tau)\right|^2 \qquad (8)$$

where Γ is the mutual intensity given by

$$\Gamma(\bar{P}_1, \bar{P}_2, \bar{V}_T) = \left(\frac{k}{2\pi L}\right)^2 \frac{1}{\pi L^2} \exp\left[\frac{ik}{2L}\left(P_1^2 - P_2^2\right)\right]$$

$$\cdot \int d\bar{\rho}_1 \exp\left[\frac{ik}{L}\left(\bar{\rho}_1 \cdot \bar{P}\right) - \frac{1}{2} D_{\psi'}(\bar{P}, o, \bar{V}_T)\right]$$

$$\cdot \iint d\bar{r}_1 \, d\bar{r}_2 \exp\left[-\frac{(r_1^2 + r_2^2)}{2a_o^2} + \frac{ik}{L} \bar{\rho}_1 \cdot \bar{r}\right.$$

$$\left. - \frac{1}{2} D_{\psi}(o, \bar{r}, \bar{V}_T)\right] \qquad (9)$$

and where $\bar{P}_1$ and $\bar{P}_2$ are the location of the two detectors in the transmitter/receiver plane, $\bar{P} = \bar{P}_2 - \bar{P}_1$, $\bar{r} = \bar{r}_2 - \bar{r}_1$ and the wave structure functions D_ψ and D_ψ' correspond to propagation from the transmitter to the target and vice versa respectively. The wave structure function is given by

$$D_\psi(\bar{\rho}, \bar{r}, \bar{V}_T) = \langle \exp[\psi^*(\bar{\rho}_2, \bar{r}_2, t_2) + \psi(\bar{\rho}_1, \bar{r}_1, t_1)] \rangle$$

$$= 2.91 \, Lk^2 \int_o^1 C_n^2(w) \left| w\bar{\rho} + (1-w)\,\bar{r} - \bar{V}_T \right|^{5/3} dt$$

In developing Eq.(9) $\bar{r}$, $\bar{\rho}$, and $\bar{P}$ were used to designate the coordinates in the transmitter, target and receiver planes respectively and were all expressed in the transmitter coordinate system. It should be noted that the coordinates at the target were not reversed after scattering from the target in deriving Eq.(9).

Eq.(9) can be evaluated by first performing the $d\bar{\rho}_1$ integration. This yields after making the change of variables

$\bar{r}_2 - \bar{r} = \bar{r}$ and $\bar{r}_2 + \bar{r}_1 = 2\bar{R}$

$$\Gamma(\bar{P}_1, \bar{P}_2, \bar{V}\tau) = \frac{U_o^2}{\pi L^2} \exp\left[\frac{ik}{2L}(P_1^2 - P_2^2) - D_{\psi'}(\bar{P}, o, \bar{V}\tau)\right]$$

$$\cdot \int d\bar{R} \int d\bar{r}\, \delta(\bar{P}+\bar{r}) \exp\left[-\frac{(2R^2 + r^2/2)}{2a_o^2} - \frac{1}{2} D_{\psi}(o, \bar{r}, \bar{V}\tau)\right] \qquad (10)$$

where use has been made of

$$\int d\theta_{\rho_1} \exp\left[\frac{ik}{L} \bar{\rho}_1 \cdot (\bar{P}+\bar{r})\right] = 2\pi J_o\left(\frac{k}{L} \rho_1 \left|\bar{P}+\bar{r}\right|\right) \qquad (11)$$

and

$$\int \rho_1 J_o\left(\frac{k}{L} \rho_1 \left|\bar{P}+\bar{r}\right|\right) d\rho_1 = 2\pi \left(\frac{L}{k}\right)^2 \delta(\bar{P}+\bar{r}) \qquad (12)$$

The $d\bar{R}$ integrations are now easily made and the final result is

$$\Gamma(\bar{P}_1, \bar{P}_2, \bar{V}\tau) = \frac{U_o^2 a_o^2}{L^2} \exp\left[\frac{ik}{2L}(P_1^2 - P_2^2)\right.$$

$$\left. - \frac{1}{2} D_{\psi'}(\bar{P}, o, \bar{V}\tau) - \frac{1}{2} D_{\psi}(o, -\bar{P}, \bar{V}\tau) - P^2/4a_o^2\right] \qquad (13)$$

Equation (13) will be evaluated using Eq.(2) which is the proposed relationship between ψ and ψ' and also Eq.(1). Using these expressions, the relationships for the wave structure functions become

$$D_{\psi}(o,-\overline{P},\overline{V}_T) = D_{\psi}(-\overline{P},o,-\overline{V}_T) = D_{\psi}(\overline{P},o,\overline{V}_T) \quad (14)$$

and

$$D_{\psi}(o,-\overline{P},\overline{V}_T) = D_{\psi}(-\overline{P},o,\overline{V}_T) = D_{\psi}(\overline{P},o,-\overline{V}_T) \quad (15)$$

respectively. The time lagged covariance is plotted in Figure 3 for the two cases. The shape of the curves is similar, but the curve for the case using Eq.(2) has its peak shifted from the origin in the direction of positive τ for positive crosswind. It would shift the opposite direction for negative crosswind. However the curve for the other case does not shift with the crosswind. It appears then that shifting or not shifting of the peak of the time-lagged covariance with the crosswind should provide a good test of validity for the use of Eq.(2) in single ended time lagged problems.

Figures 4 and 5 show typical experimental data for the time-lagged covariance with the crosswind in opposite directions. As can be seen, the peaks shift as predicted for the case corresponding to Eq.(2) and this along with the analysis leads us to conclude that Eq.(2) is the proper relation to be used in problems of this type.

Acknowledgement

This work was supported in part by the Army Research Office under Contract DAAG 29-83-K-0077 and the National Science Foundation under Grant Number ECS-8300221.

References

1. R. F. Lutomirski and H. T. Yura, "Propagation of a finite optical beam in an inhomogeneous medium," Appl. Opt. 10, 1652 (1971).

2. Jeffrey H. Shapiro, "Reciprocity of the turbulent atmosphere," J. Opt. Soc. Am. 61, 492 (1971).

3. M. H. Lee, J. F. Holmes and J. R. Kerr, "Statistics of speckle propagation through the turbulent atmosphere," J. Opt. Soc. Am. 66, 1164-1172 (1976).

4. Steve F. Clifford and Stephen Wandzura, "Monostatic heterodyne lidar performance: the effect of the turbulent atmosphere," Appl. Opt. 20, 514 (1981).

5. J. H. Shapiro, B. A. Capron, and R. C. Harney, "Imaging and target detection with a heterodyne-reception optical radar," Appl. Opt. 20, 3292 (1981).

6. Barry J. Rye, "Refractive-turbulence contribution to incoherent backscatter heterodyne lidar returns," J. Opt. Soc. Am. 71, 687 (1981).

7. William C. Meecham, "Relation Between Time Symmetry and Reflection Symmetry of Turbulent Fluids," The Physics of Fluids 1, 408 (1958).

8. S. F. Clifford, Laser Beam Propagation in the Atmosphere - Chapter Two, Springer-Verlag, New York, 1978.

9. V. I. Tatarskii, The Effects of the Turbulent Atmosphere on Wave Propagation, U.S. Dept. of Commerce, Springfield, VA, 1971.

Figure Captions

1. Wind sensing using a correlation detector in the line of sight case.
2. Path geometry and the coordinate systems used.
3. Normalized time delayed covariance of the intensity of a target generated speckle pattern versus time delay in the turbulent atmosphere with and without wind reversal; Theory.
4. Normalized time delayed covariance of intensity of a target generated speckle pattern versus time delay in the turbulent atmosphere; Experimental data using a CO_2 heterodyne system.
5. Same as 4.

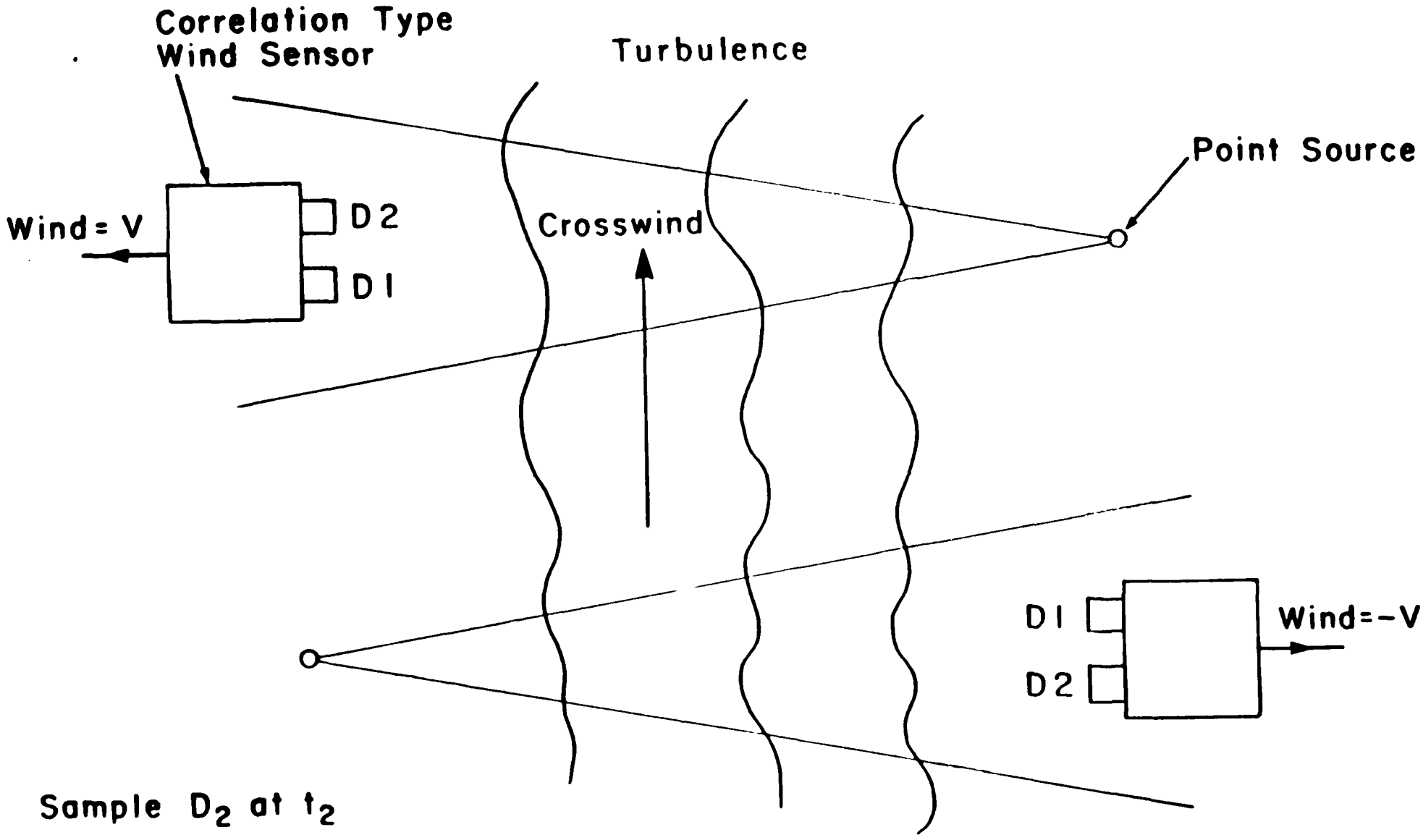
Correlation Type
Wind Sensor
Turbulence
Point Source
Wind = V
D2
D1
Crosswind
D1
D2
Wind=-V
Sample D_2 at t_2
Sample D_1 at t_1
$t_2 > t_1$

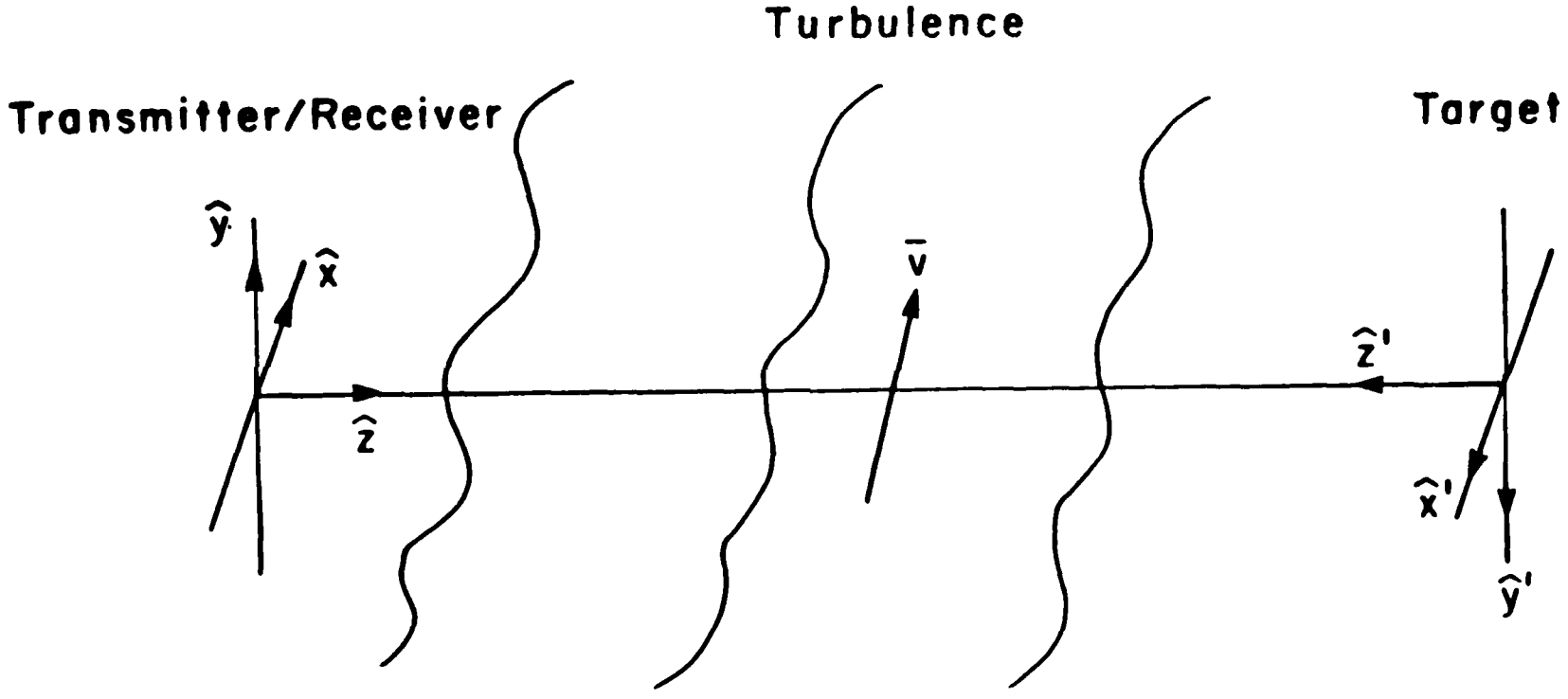
Turbulence
Transmitter/Receiver
Target
$\hat{y}$
$\hat{x}$
$\hat{z}$
$\bar{v}$
$\hat{z}'$
$\hat{x}'$
$\hat{y}'$

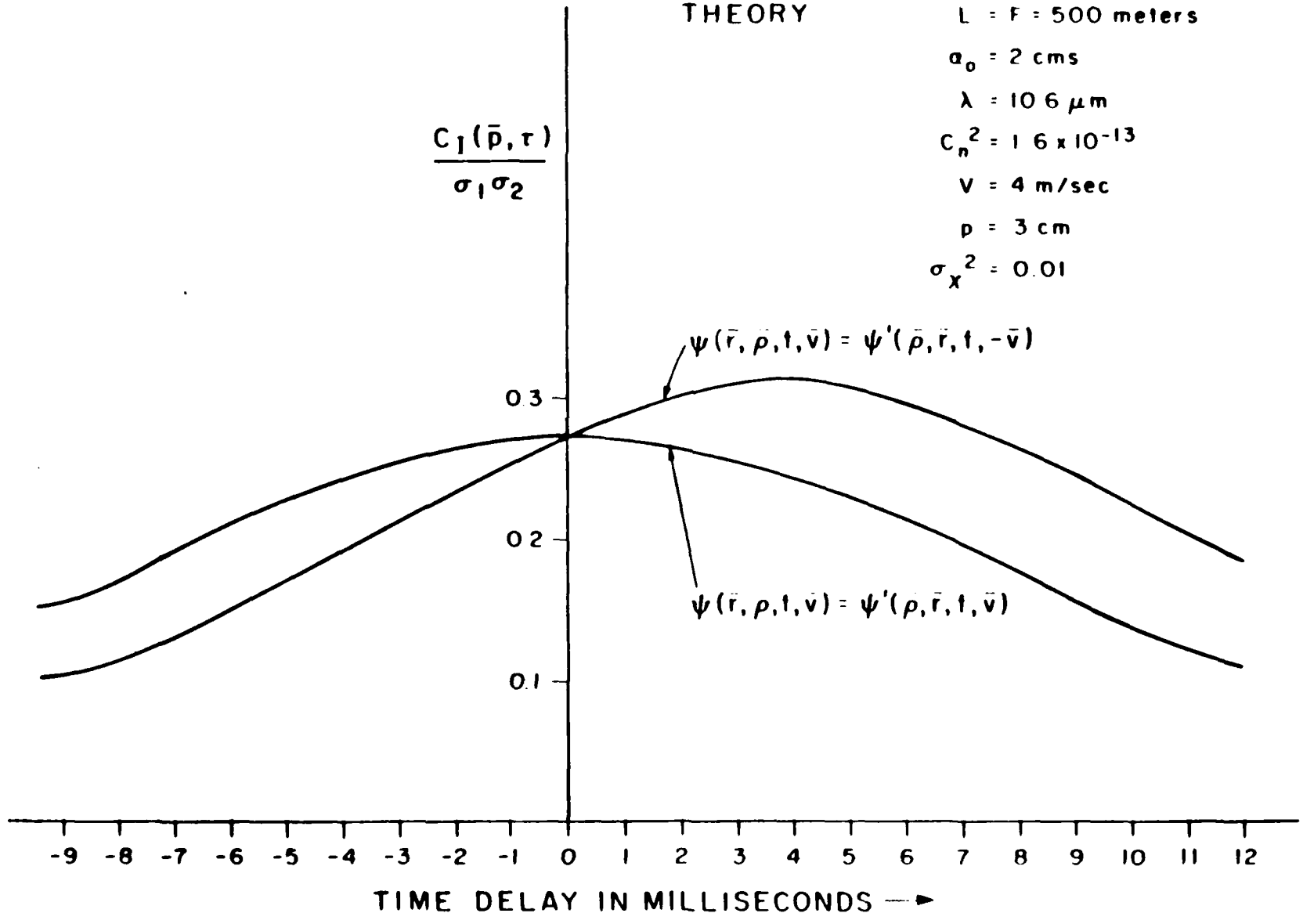
THEORY
L = F = 500 meters
a_0 = 2 cms
λ = 10 6 μm
C_n^2 = 1 6 x 10^{-13}
V = 4 m/sec
p = 3 cm
σ_x^2 = 0.01
$\frac{C_I(\bar{\rho},\tau)}{\sigma_1\sigma_2}$
$\psi(\bar{r},\bar{\rho},t,\bar{v}) = \psi'(\bar{\rho},\bar{r},t,-\bar{v})$
$\psi(\bar{r},\rho,t,\bar{v}) = \psi'(\rho,\bar{r},t,\bar{v})$
0.3
0.2
0.1
-9 -8 -7 -6 -5 -4 -3 -2 -1 0 1 2 3 4 5 6 7 8 9 10 11 12
TIME DELAY IN MILLISECONDS

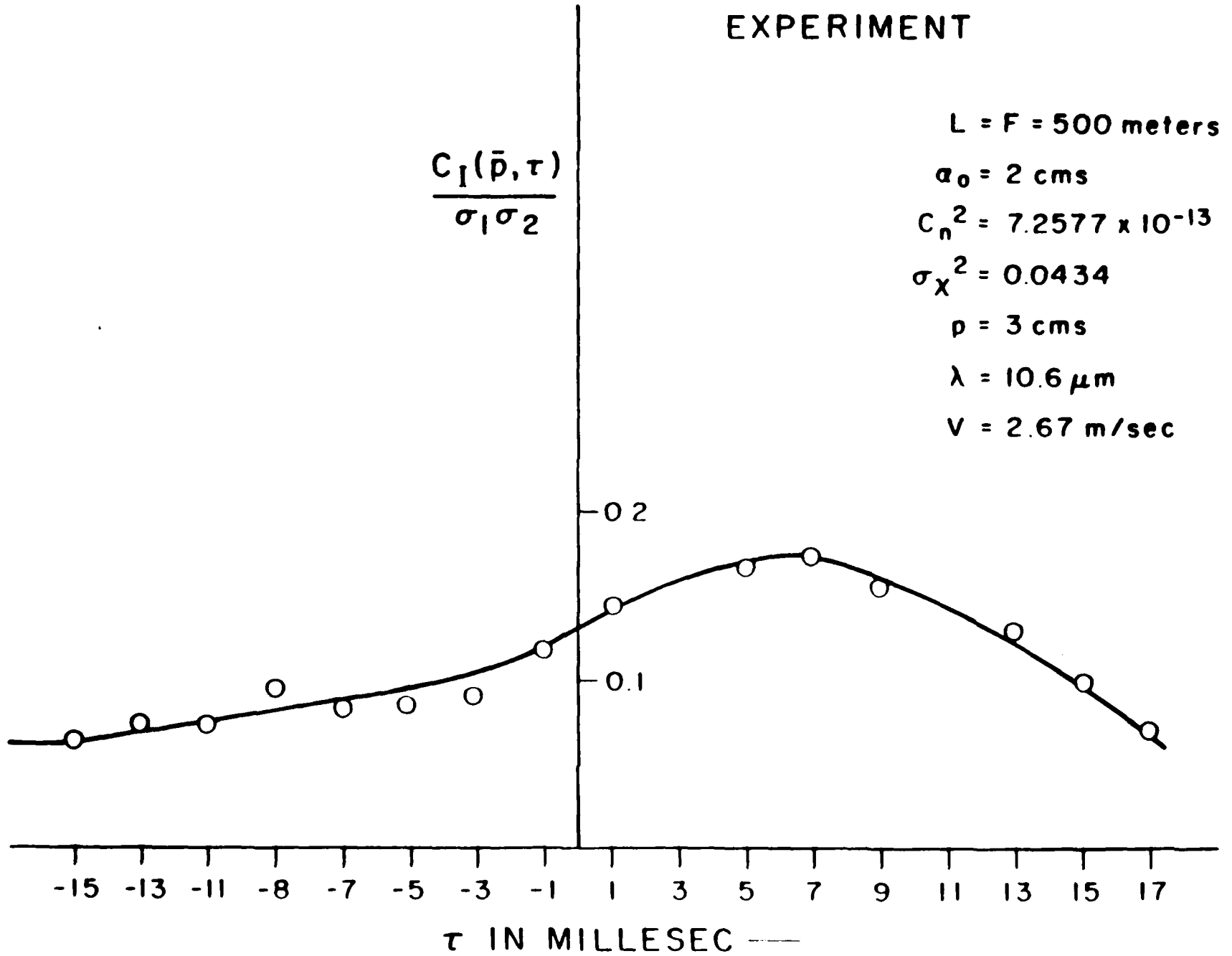
EXPERIMENT
$\frac{C_I(\bar{p},\tau)}{\sigma_1\sigma_2}$
L = F = 500 meters
a_0 = 2 cms
C_n^2 = 7.2577 x 10^{-13}
σ_χ^2 = 0.0434
p = 3 cms
λ = 10.6 μm
V = 2.67 m/sec
0.2
0.1
-15 -13 -11 -8 -7 -5 -3 -1 1 3 5 7 9 11 13 15 17
τ IN MILLESEC

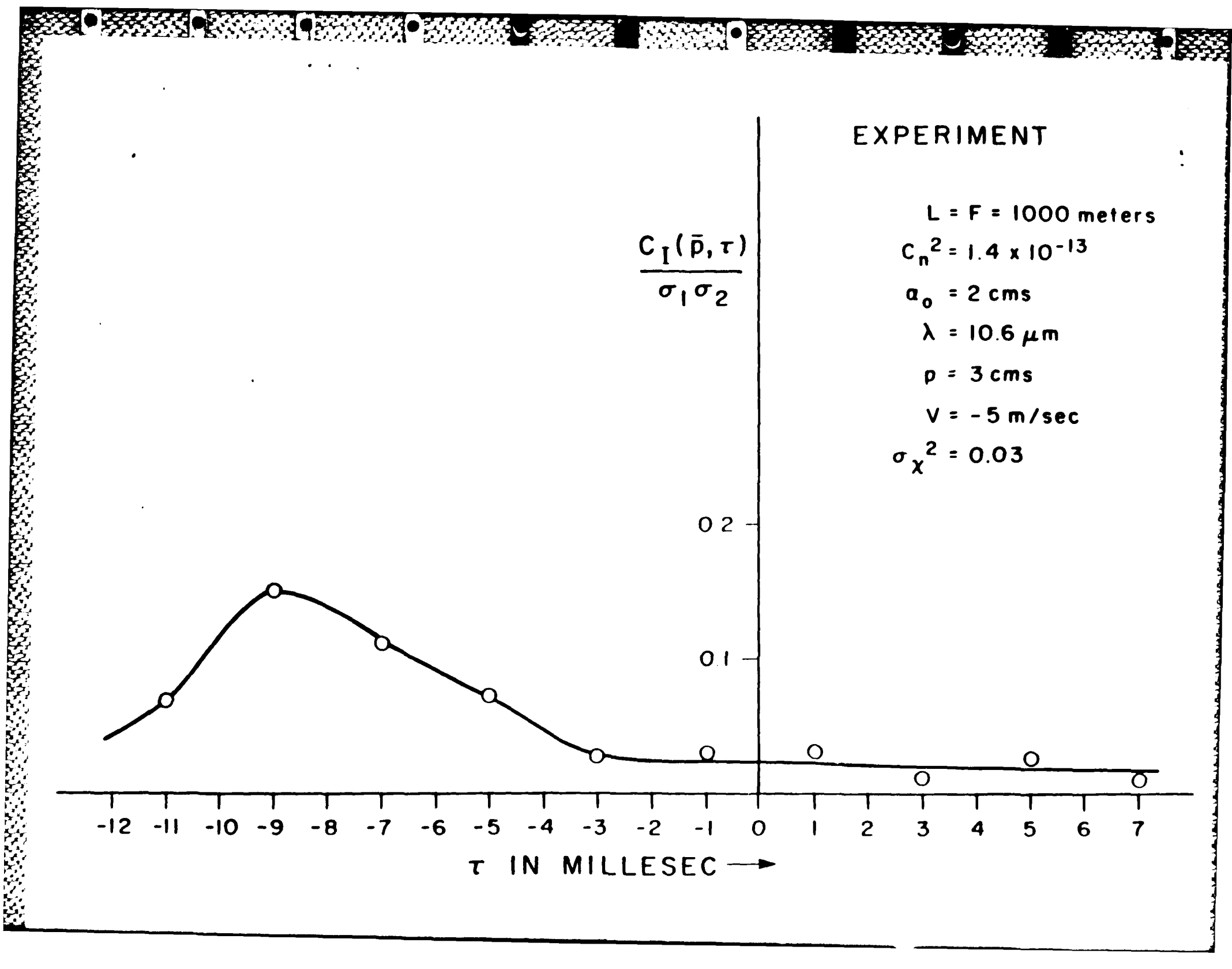
EXPERIMENT
L = F = 1000 meters
$C_n^2 = 1.4 \times 10^{-13}$
a_o = 2 cms
λ = 10.6 μm
p = 3 cms
V = -5 m/sec
$\sigma_\chi^2 = 0.03$
$\frac{C_I(\bar{p},\tau)}{\sigma_1\sigma_2}$
0.2
0.1
-12 -11 -10 -9 -8 -7 -6 -5 -4 -3 -2 -1 0 1 2 3 4 5 6 7
τ IN MILLESEC →

SUMMARY (200 words maximum)

TYPE ENTIRE MANUSCRIPT, INCLUDING ANY REFERENCES, DOUBLE SPACE IN A SINGLE PARAGRAPH. ADDRESS SHOULD BE AS BRIEF AS POSSIBLE, BUT SUFFICIENT FOR POSTAL SERVICE. DO NOT USE ABBREVIATIONS.

Remote crosswind measurement using speckle-turbulence interaction and optical heterodyne detection[1]
(Title of paper Capitalize only the first letter of each principal word.)

J. Fred Holmes, Farzin Amzajerdian, V. S. Rao Gudimetla, John M. Hunt
(Author)

Applied Physics and Electrical Engineering
(Department)

Oregon Graduate Center
(Institution)

19600 N.W. Von Neumann Dr. (Number) (Street) Beaverton, OR (City) (State) 97006-1999 (Zip)

Speckle-turbulence interaction has the potential for allowing single ended remote sensing of the path averaged vector crosswind in a plane perpendicular to the line of sight to a target. If a laser transmitter is used to illuminate a target, the resultant speckle field generated by the target is randomly perturbed by the atmospheric turbulence as it propagates back to the location of the transmitter-receiver. When a crosswind is present, this scintillation pattern will move with time across the receiver aperture; and consequently, the time delayed statistics of this turbulence perturbed speckle field are dependent on the crosswind velocity. A continuous wave (cw) laser transmitter of modest power level in conjunction with optical heterodyne detection can be used to exploit the speckle-turbulence interaction and measure the crosswind. The use of a cw transmitter at 10.6 microns and optical heterodyne detection has many advantages over previous work which used direct detection and a double pulsed source in the near infrared. These advantages include the availability of compact, reliable and inexpensive transmitters; better penetration of smoke, dust and fog; stable output power; no beam pointing jitter; and considerably reduced complexity in the receiver electronics. In addition, with a cw transmitter, options exist for processing the received signals for the crosswind that do not require a knowledge of the strength of turbulence. Analytical and experimental results will be presented.

[1]This material is based in part upon work supported by the Army Research Office under contract DAAG29-83-K-0077.

Speckle propagation through turbulence: its characteristics and effects

J. Fred Holmes
Department of Applied Physics and Electrical Engineering, Oregon Graduate Center
19600 N. W. Walker Road, Beaverton, Oregon 97006

Abstract

Atmospheric turbulence and target induced speckle can have a significant and deleterious effect on the performance of optical systems. The primary effect is to introduce a strong fluctuation in the intensity and a random perturbation of the phase of the fields at the optical receiver. This is equivalent to introducing a large noise source at the receiver; and consequently multiple samples and/or clever processing techniques are needed to accurately estimate the magnitude of the received intensity. In addition, for coherent detection schemes, the random phase and finite transverse coherence length introduced by the speckle and turbulence will limit the size of aperture that can be used. These characteristics of the speckle field after propagation through turbulence and its effect on optical systems will be discussed in a tutorial overview.

Introduction

Atmospheric turbulence and target induced speckle can have a significant and deleterious effect on the performance of optical systems that operate in or through the turbulent atmosphere. Figure 1 shows a typical system arrangement.

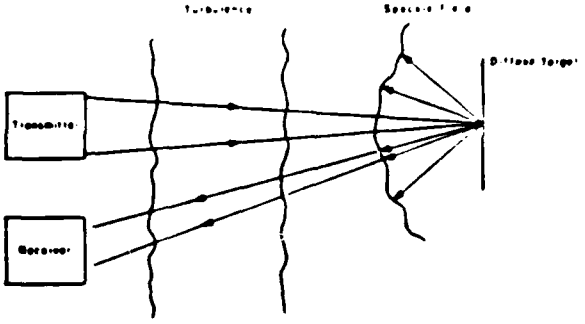

Figure 1. Typical system configuration.

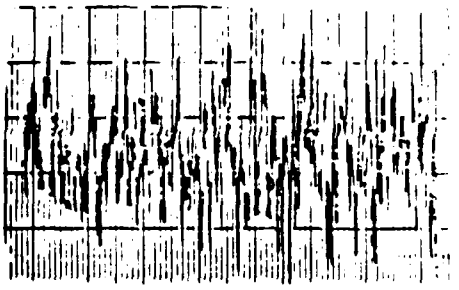

Figure 2. Signal contaminated by speckle with unity contrast ratio.

The source is a TEM_{oo} laser beam that propagates through the atmospheric turbulence to a diffuse target. The turbulence will degrade the spatial coherence of the beam, introduce amplitude fluctuations and cause the beam to wander over the target surface. The diffuse surface will completly destroy the spatial coherence of the beam and generate a speckle field that will then propagate back through the turbulence to the receiver. The primary effects at the receiver are a strong fluctuation in the intensity and a random perturbation of the phase of the fields. This is equivalent to introducing a large noise source at the receiver and consequently multiple samples and/or clever processing techniques are needed to accurately estimate the magnitude of the received intensity. In addition, for coherent detection schemes, the random phase and finite transverse coherence length introduced by the speckle and turbulence will limit the size of aperture that can be used.

Background

Before discussing the combined effects of speckle and turbulence, some background on speckle statistics will be presented to give the reader a better feel for the speckle problem before the combined effects of speckle and turbulence are introduced. The statistical parameters that are important are the normalized variance, which is a measure of the degree of signal fluctuation, the covariance, from which the transverse correlation length can be derived, and the probability density function. For a monochromatic laser source, a diffuse target, and no turbulence the normalized variance of the received intensity is equal to unity[1] and is defined as

$$\sigma_{I_N}^2 = \frac{\langle (I - \langle I \rangle)^2 \rangle}{\langle I \rangle^2} \tag{1}$$

A sample function for this type of signal is shown in Figure 2 where the horizontal axis is time or space and the vertical axis is the received intensity. In the former case there must be relative motion between the incident beam and the target. Otherwise the signal for any particular sample function would be constant in time. There would however be a substantial variation in signal level between the sample functions making up a complete ensemble. Equation (1) is the result of taking an ensemble average. However, the same result would be obtained if the sample function in Figure 2 were averaged to obtain the mean and variance. In any case, the speckle with its unity normalized variance constitutes a strong source of random noise in the system.

The normalized covariance of the received intensity is defined as

$$C_{I_N}(\rho) = \frac{\langle (I(\bar{\rho}_2) - \langle I \rangle)(I(\bar{\rho}_1) - \langle I \rangle) \rangle}{\sigma_I^2} \tag{2}$$

where $\bar{\rho} = \bar{\rho}_2 - \bar{\rho}_1$

and in the absence of turbulence can be expressed as[2]

$$C_{I_N}(\bar{\rho}) = \exp\left\{ -\frac{\rho^2}{2} \left[\frac{1}{\sigma_0^2} + \left[\frac{k}{L} \sigma_0 \left(1 - \frac{L}{F} \right) \right]^2 \right] \right\} \tag{3}$$

where σ_0 is the illuminating beam radius at the transmitter, ρ is the spacing between detectors, L is the path length, F is the distance at which the transmitter is focused and k is the wave number. It can be seen that for a focused transmitter, the speckle size back at the receiver is approximately the same size as the transmitted beam. As the focus distance F is increased, the spot size on the target grows and the speckle size back at the receiver decreases continuously.

The speckle scale size is important if aperture averaging is used to reduce the variance of the received signal. Each speckle can be thought of as being independent of all the other speckles. Consequently, what the collection aperture does then is add up the intensities from each speckle and since they are independent, the variance goes down as 1/N where N is the number of independent speckles. This effect can be estimated using the covariance scale size and the aperture size to find an approximate N; or an exact calculation can be performed.[1]

Turbulence and Speckle

When turbulence is present, an additional fluctuation is introduced in the signal at the receiver in addition to that caused by speckle. This is illustrated[2] in Figure 3 which shows the normalized variance of the received intensity versus the Rytov variance which is the normalized variance as observed by a point detector located at the receiver due to a point source at the target. As can be seen from the figure, the normalized variance increases up to a Rytov variance of around 0.1 and then decreases until it reaches unity again. The maximum increase is around 25 percent. Detailed formulations from which the variance can be calculated are contained in Reference 2. It should be noted however that the results for different path lengths, beam sizes and wavelengths do not differ much from that shown in Figure 3. The Rytov variance is given by

$$\sigma_R^2 = 0.124\, k^{7/6} L^{11/6} C_n^2 \tag{4}$$

where C_n^2 represents the strength of turbulence (structure parameter).

There is an additional effect that can increase the variance beyond that predicted in Figure 3. If the beam wanders on and off the target or wanders around on a target of greatly varying reflectivity, the variance can increase markedly.[3] This wander can be caused by the atmospheric turbulence or by beam jitter in the transmitter system.

In order to evaluate the effects of aperture averaging, the decorrelation due to separation of samples in space and/or time, and the transverse phase coherence length, the time delayed covariance is needed. At lower values of integrated path turbulence

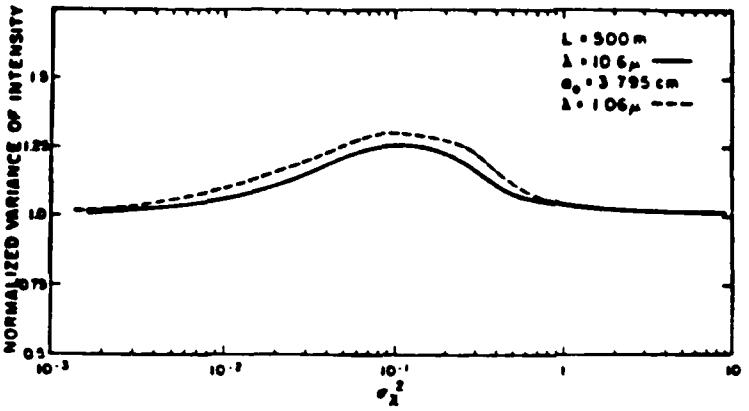

Figure 3. Normalized variance of the received intensity versus the log-amplitude variance, focused beam, 500-m range, 1.06- and 10.6-μm wavelengths, a_0 = 3.795 cm.

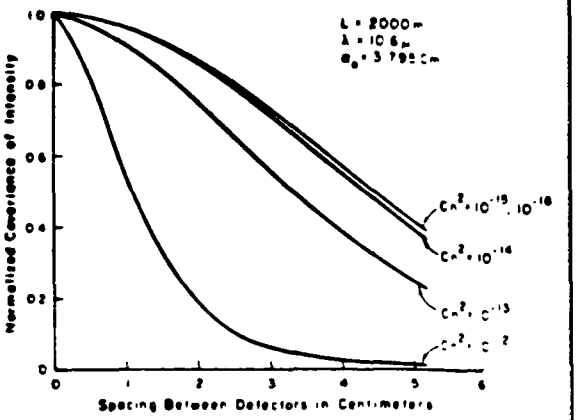

Figure 4. Normalized covariance of the received intensity, focused beam, 2000-m range, 10.6-μm wavelength, a_0 = 3.795 cm.

($\sigma_1^2 < 0.003$), a very simple analytic formulation for the time delayed covariance can be used. It is given for the case of uniform turbulence along the path by

$$C_I(\bar{\rho},\bar{V}\tau) = \langle I\rangle^2 \exp\left[-\frac{1}{2}\left[\frac{1}{\rho_0^2} + \left(\frac{ka}{L}\right)^2 (1 - L/F)^2\right]\rho^2\right]$$

$$\exp\left[-5.82\ Lk^2C_n^2 \int_0^1 |(1-t)\bar{\rho} - \bar{V}\tau|^{5/3}\, dt\right] \qquad (5)$$

where ρ_0 the transverse phase coherence length is given by

$$\rho_0 = (0.545625\ C_n^2\ Lk^2)^{-3/5}$$

$\bar{V}$ is the vector crosswind, and τ is the time delay between samples. It should be noted that Equation (5) does not include the effects of the log-amplitude perturbation and therefore is not complete. Consequently some care should be exercised in its use. For instance, Equation (5) predicts that the normalized variance ($C_I(0,0)/\langle I\rangle^2$) is unity independent of turbulence level whereas the more complete formulation[2] which includes the log-amplitude perturbation gives the result (verified by experiment) shown in Figure 3. A more complete but considerably more complicated formulation is available[2] that includes the log-amplitude perturbation. Using it, numerical data for the covariance curves shown in Figure 4 was generated. As discussed in the previous section, there is a target induced speckle scale size that for a given scenario is fixed (10^{-16} curve). However, when turbulence is present, this scale size is dynamic and as illustrated in Figure 4 decreases as the strength of turbulence increases.

Figure 5 shows experimental and numerical data (using the complete theory) for the time delayed covariance function,[5,6] which can be used to estimate the degree of correlation between samples that are separated in space and time. Using Equation (5) ($\sigma_1^2 < 0.003$), the autocovariance for the received intensity can be obtained. It is given by

$$C_I(o,\bar{V}\tau) = \langle I\rangle^2 \exp\left[-10.67\left(\frac{V\tau}{\rho_0}\right)^{5/3}\right] \qquad (6)$$

It should be noted that both the time-delayed covariance and the autocovariance depend on the crosswind velocity and the strength of turbulence. The Fourier transform of Equation (6) yields the power spectral density for the received intensity which is plotted in Figure

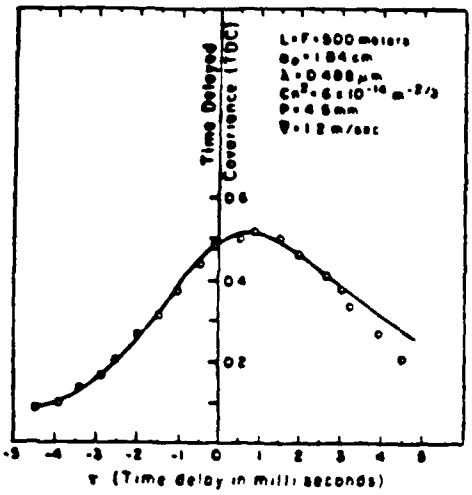

Figure 5. Time delayed covariance, numerical and experimental data.

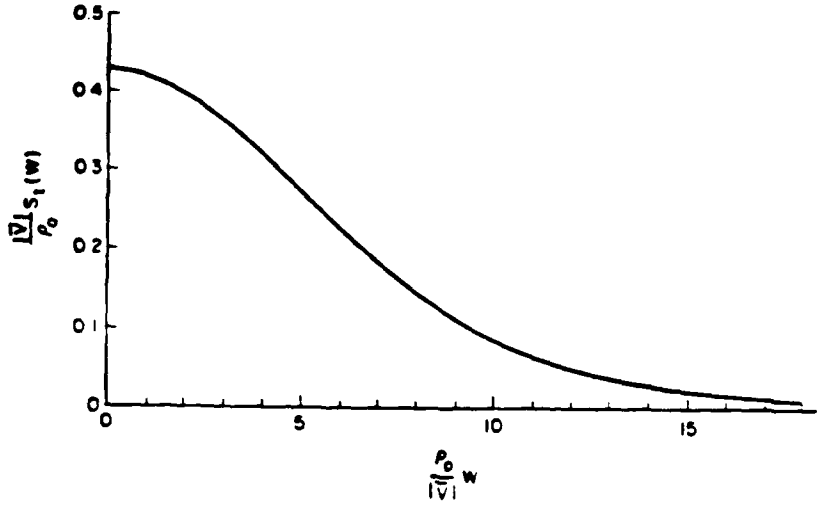

Figure 6. Temporal, power spectral density, received intensity.

6. It can be used to estimate the bandwidth requirements for experimentally measuring the speckle-turbulence statistics ($\sigma_x^2 < 0.003$).

In estimating the effect that turbulence and speckle will have on system performance, the probability density function (PDF) is useful. For a monochromatic source, a diffuse target, and no turbulence, at the receiver the fields have a Gaussian distribution, the field amplitude has a Rayleigh distribution, and the intensity has an exponential distribution. Turbulence will modify these distributions. However, for integrated path turbulence corresponding to Rytov variances less than 0.003, they are a reasonable approximation. Figure 7 shows experimental cumulative PDF data for Rytov variances of 0.0022 and 0.1735. At the lower value, the data matches the experimental distribution quite well. However at the higher turbulence level there is substantial deviation from exponential. Analytical and experimental work [8,9] has shown that for a fully developed Gaussian speckle pattern, the PDF of the intensity changes from an exponential density function at zero turbulence to a K distribution as the turbulence level increases. The PDF is given by

$$P_I(a) = 2\left(\frac{M}{\lambda}\right)^{\frac{M+1}{2}} \frac{a}{\Gamma(M)}^{\frac{M-1}{2}} K_{M-1}\left(2\sqrt{\frac{Ma}{\lambda}}\right) \qquad (7)$$

where K_{M-1} is the modified Bessel function of order M-1, λ equals $\langle I \rangle$, and M equals $2/(\sigma_{I_N}^2 - 1)$ Figure 8 shows numerical data using Equation (7) and experimental data for the cumulative PDF. Good agreement was obtained. The parameter M can be obtained in terms of the path length, wavelength, beam size and strength of turbulence using Reference 2. Formulations for the PDF with turbulence effects are also available [8] for partially developed speckle, speckle with a coherent background (glints), and polychromatic speckle.

Beam jitter can contribute both to temporal fluctuations of the signal and to decorrelation between signal samples. A measure of the magnitude of this effect can be obtained from the crosscorrelation, $C_I(o,\tau)$, between samples separated in time. Figure 9 shows some experimental data taken using a pulsed Nd:YAG laser.

The crosscorrelation (normalized to $\langle I \rangle^2$) was measured for the received signals from two successive pulses spaced one millisecond apart. If the beams corresponding to the two pulses are perfectly aligned, then they will go through the same portion of the atmosphere, strike the same spot on the target and generate a unity normalized crosscovariance back at the receiver. However, if the beams have a static or dynamic misalignment, the signals will decorrelate and the crosscovariance will decrease to a value less than unity. As can be seen from Figure 9, there appears to be considerable static and dynamic misalignment of the laser transmitter used in the experiment. This was confirmed by experiments on the laser transmitter. The misalignment problem has been analyzed and formulations are available [10] which include the effects of static and dynamic beam misalignment. Figure 10 shows some numerical data using these formulations for the dynamic misalignment case. The

parameter β is defined to be the ratio of the beam misalignment angle corresponding to 84 percent cumulative probability to the beam divergence angle in vacuum.

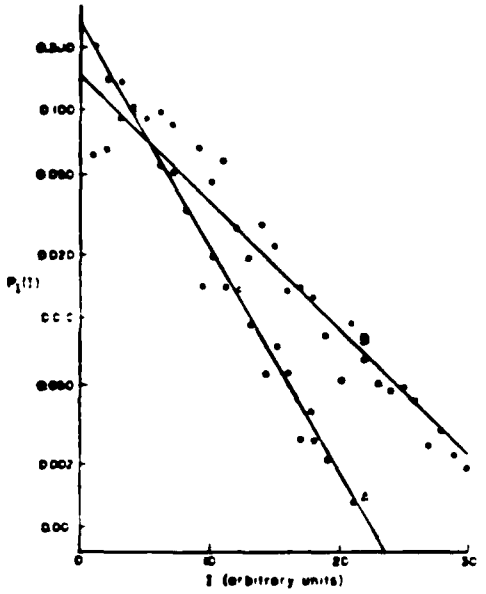

Figure 7. Probability distribution functions of the received irradiance seen in two turbulence conditions. (a) O_i experimental data from low turbulence: $C_n^2 = 1.0 \times 10^{-15}$ $m^{-2/3}$, L = 500 m, $\sigma_{I_N}^2 = 1.02$. (b) •, experimental data: $C_n^2 = 8.0 \times 10^{-14}$ $m^{-2/3}$, L = 500 m, $\sigma_{I_N}^2 = 1.2$. The solid lines indicate exponential distributions of the same means as the experimental points.

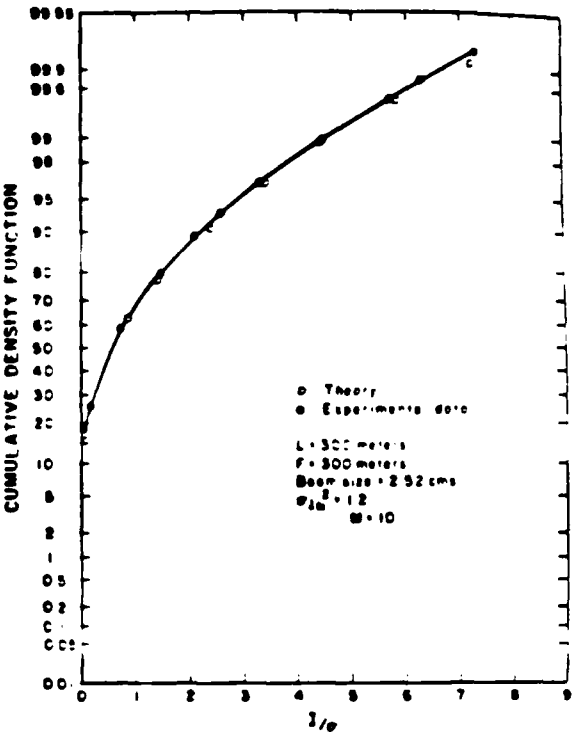

Figure 8. Comparison of experimental cumulative PDF with theory for a monochromatic speckle pattern, 300-m path length.

It should be noted that changing the wavelength between measurements can have the same effect as moving the spot on the target in that it changes the speckle pattern and decorrelates the signals. This is a target dependent phenomenon; and in general if $\Delta\omega \ll \sigma_\omega$, where σ_ω is the standard deviation of the target surface roughness and $\Delta\omega$ is the change in frequency, then the pattern does not change very much and the signals will be highly correlated.

References

1. Dainty, J. C., Laser Speckle and Related Phenomena (Springer-Verlag, 1975).
2. Holmes, J. Fred, Lee, Myung Hun, and Kerr, J. Richard, "Effect of the log-amplitude covariance function on the statistics of speckle propagation through the turbulent atmosphere," J. Opt. Soc. Am. 70, May 1981.
3. McIntyre, C. M., Lee, Myung Hun, and Churnside, J. H., "Statistics of irradiance scattered from a diffuse target containing multiple glints," J. Opt. Soc. Am. 70, September 1980.
4. Lee, Myung Hun, Holmes, J. Fred, and Kerr, J. Richard, "Statistics of speckle propagation through the turbulent atmosphere," J. Opt. Soc. Am. 66, November 1976.
5. Gudimetla, V. S. Rao, and Holmes, J. Fred, "Time delayed covariance of the received intensity for a target generated speckle pattern in the turbulent atmosphere," Annual Meeting of the Optical Society of America, Tucson, Arizona, October 18-22, 1982.

6. Gudimetla, V. S. Rao, "Statistics of Polychromatic Speckle Propagation Through the Turbulent Atmosphere," Ph.D. Dissertation, Department of Applied Physics and Electrical Engineering, Oregon Graduate Center, 1982.

7. Pincus, Philip A., Fossey, Michael E., Holmes, J. Fred, and Kerr, J. R., "Speckle propagation through turbulence - experimental," J. Opt. Soc. Am. 68, June 1978.

8. Gudimetla, V. S. Rao, and Holmes, J. Fred, "Probability density function of the intensity for a laser generated speckle field after propagation through the turbulent atmosphere," J. Opt. Soc. Am. 72, September 1982.

9. Gudimetla, V. S. Rao, and Holmes, J. Fred, "Probability density function of the intensity for a laser generated speckle pattern in the turbulent atmosphere," Annual Meeting of the Optical Society of America, Kissimmee, Florida, October 26-30, 1981.

10. Lee, Myung Hun, and Holmes, J. Fred, "Speckle intensity crosscovariance function for two misaligned laser beams in a turbulent atmosphere," J. Opt. Soc. Am. 70, May 1981.

11. Holmes, J. Fred, and Gudimetla, V. S. Rao, "Variance of intensity for a discrete spectrum, polychromatic speckle field after propagation through the turbulent atmosphere," J. Opt. Soc. Am. 71, October 1981.

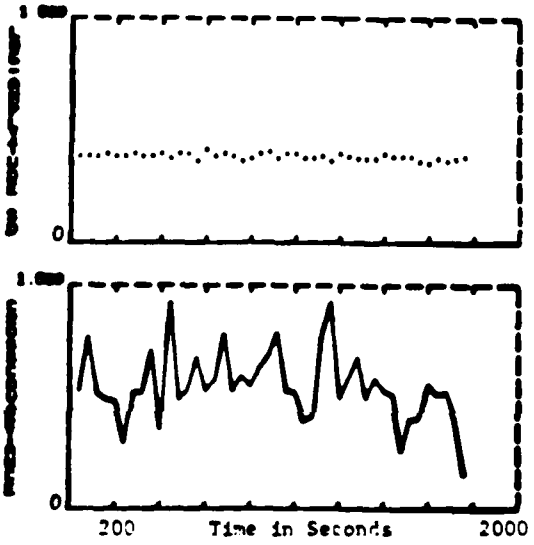

Figure 9. Crosscovariance, Target Range = 1600 m, Time Delay = 10^{-3} s, Average Crosswind = 3 m/s, average σ_x = 0.38, λ = 1.06 microns, 40 samples per data point.

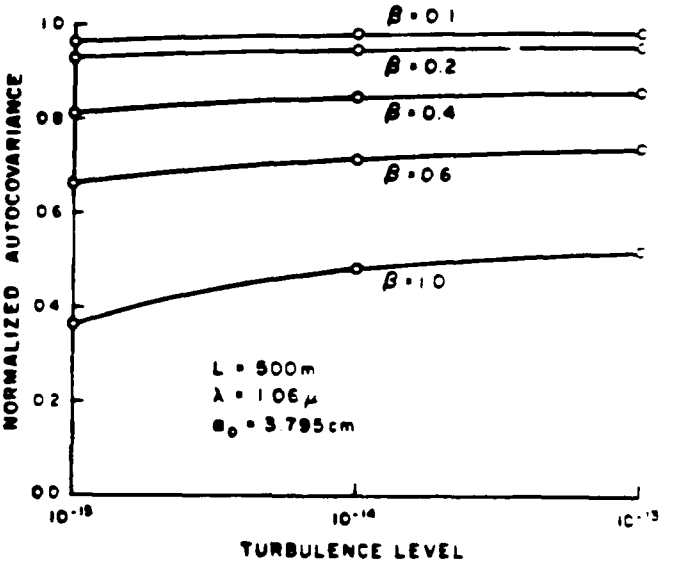

Figure 10. Normalized autocovariance of a randomly misaligned laser beam versus C_n^2. Focused beam, 500-m range, 1.06-μm wavelength, a_0 = 3.795 cm.

Acknowledgment

This work has been supported in part by:

U. S. Air Force Weapons Laboratory and the U. S. Army Atmospheric Sciences Laboratory, White Sands Missile Range under Contract DAA D07-74-C-0094.

Frankford Arsenal, Philadelphia, Pennsylvania under Contract DAAA 25-76-C0132.

U. S. Army Armament Research and Development Command under Contract DAAK 10-78-Q-0093.

U. S. Army Atmospheric Sciences Laboratory, White Sands Missile Range, under Contract DAA-D07-79-R-0137.

U. S. Army Research Office under Contract DAAG 29-83-K-0077.

National Science Foundation under grant number ECS-8300221.

SUMMARY (200 words maximum)

TYPE ENTIRE MANUSCRIPT, INCLUDING ANY REFERENCES DOUBLE SPACE IN A SINGLE PARAGRAPH. ADDRESS SHOULD BE AS BRIEF AS POSSIBLE, BUT SUFFICIENT FOR POSTAL SERVICE. DO NOT USE ABBREVIATIONS.

Time Lagged Reciprocity in the Turbulent Atmosphere[1]
(Title of paper. Capitalize only the first letter of each principal word.)

V. S. Rao Gudimetla and J. Fred Holmes
(Author)

Department of Applied Physics and Electrical Engineering, Oregon Graduate Center
(Department) (Institution)

19600 N.W. Walker Road Beaverton OR 97006
(Number) (Street) (City) (State) (Zip)

In single ended optical propagation problems, the transmitter and receiver are located at the same end of the propagation path. The transmitted radiation propagates down the path and strikes a target where it is scattered or reflected back towards the receiver. The radiation interacts with the atmospheric turbulence on both the down and back paths. In analyzing this type of problem, a reciprocity relationship for the point spread function is very useful. For the non-time lagged case, there is a well known reciprocity relationship and it would seem that Taylor's Hypothesis could be used to convert it to the time lagged case. However, for the non-time lagged case, the statistics are isotropic; but for the time lagged case the statistics depend on direction. Consequently, careful consideration must be given to the coordinate system used to describe the propagation on each path. A time lagged point spread function will be developed and experimental evidence presented to support the result.

[1]This material is based in part upon work supported by the Army Research Office under Contract DAAG 29-83-K-0077 and the National Science Foundation under grant number ECS-8300221.

THE EFFECTS OF TARGET AND SOURCE MOTION AND BEAM SLEWING ON SPECKLE PROPAGATION THROUGH TURBULENCE[1]

J. Fred Holmes and V. S. Rao Gudimetla
Department of Applied Physics and Electrical Engineering
Oregon Graduate Center
19600 N.W. Walker Road
Beaverton, OR 97006

Atmospheric turbulence and target induced speckle can have a significant and deleterious effect on the performance of optical systems. One method that is used to overcome these effects is to take averages in space and/or time. However, the reduction in signal fluctuation due to averaging are affected by target, receiver and source motion and by beam slewing. Consequently, formulations for the mutual intensity, the time delayed covariance and the power spectral density that include these effects are needed. Formulations for these statistical measures have been developed that include the effects of source, receiver and target motion and beam slewing as well as the effects of the speckle and turbulence. Utilizing the extended Huygens-Fresnel formulation, expressions for the mutual intensity, the time delayed covariance, and the power spectral density have been developed that are valid at all levels of turbulence. A TEM_{00} monochromatic laser in conjunction with a perfectly diffuse target is used to generate the speckle field. The formulations obtained are reduced to numerical data for illustrating the magnitude of the effects.

[1]This material is based in part upon work supported by the Army Research Office under Contract DAAG 29-83-K-0077 and the National Science Foundation under grant number ECS-8300221.

SUMMARY (200 words maximum)

TYPE ENTIRE MANUSCRIPT, INCLUDING ANY REFERENCES DOUBLE SPACE IN A SINGLE PARAGRAPH. ADDRESS SHOULD BE AS BRIEF AS POSSIBLE, BUT SUFFICIENT FOR POSTAL SERVICE. DO NOT USE ABBREVIATIONS.

The Effects of Target and Source Motion on Speckle Propagation Through Turbulence[1]

(Title of paper. Capitalize only the first letter of each principal word.)

J. Fred Holmes, V. S. Rao Gudimetla

(Author)

Applied Physics and Electrical Engineering, Oregon Graduate Center

(Department) (Institution)

19600 N.W. Walker Road Beaverton Oregon 97006

(Number) (Street) (City) (State) (Zip)

Atmospheric turbulence and target induced speckle can have a significant and deleterious effect on the performance of optical systems. One method that is used to overcome these effects is to take averages in space and/or time. However, the reduction in signal fluctuation due to averaging are affected by target and source motion. Consequently, formulations for the mutual intensity, the time delayed covariance and the power spectral density that include target and source motion effects are needed. Formulations for these statistical measures have been developed that include the effects of source and target motion as well as the effects of the speckle and turbulence. Utilizing the extended Huygens-Fresnel formulation and assuming that the optical fields are jointly Gaussian at the receiver, expressions for the mutual intensity, the time delayed covariance, and the power spectral density have been developed. A TEM_{oo} monochromatic laser in conjunction with a perfectly diffuse target is used to generate the speckle field. The formulations obtained are easily reduced to numerical data, but are valid only for Rytov variances less than 0.03 due to the jointly Gaussian assumption.

[1]This material is based in part upon work supported by the Army Research Office under Contract DAAG 29-83-K-0077 and the National Science Foundation under grant number ECS-8300221.

END

FILMED

3 -86

DTIC